SPECIAL REPORT

A Theory of the Podkletnov Effect based on General Relativity: Anti-Gravity Force due to the Perturbed Non-Holonomic Background of Space

Dmitri Rabounski and Larissa Borissova
E-mail: rabounski@yahoo.com; lborissova@yahoo.com

We consider the Podkletnov effect — the weight loss of an object located over a superconducting disc in air due to support by an alternating magnetic field. We consider this problem using the mathematical methods of General Relativity. We show via Einstein's equations and the geodesic equations in a space perturbed by a disc undergoing oscillatory bounces orthogonal to its own plane, that there is no rôle of superconductivity; the Podkletnov effect is due to the fact that the field of the background space non-holonomity (the basic non-othogonality of time lines to the spatial section), being perturbed by such an oscillating disc produces energy and momentum flow in order to compensate the perturbation in itself. Such a momentum flow is directed above the disc in Podkletnov's experiment, so it works like negative gravity (anti-gravity). We propose a simple mechanical system which, simulating the Podkletnov effect, is an experimental test of the whole theory. The theory allows for other "anti-gravity devices", which simulate the Podkletnov effect without use of very costly superconductor technology. Such devices could be applied to be used as a cheap source of new energy, and could have implications to air and space travel.

Contents

1 Introducing Podkletnov's experiment

In 1992, Eugene Podkletnov and his team at the Tampere Institute of Technology (Finland) tested the uniformity of a unique bulky superconductor disc, rotating at high speed via a magnetic field [1]. The 145×6-mm superconductor disc was horizontally oreinted in a cryostat and surrounded by liquid helium. A small current was initiated in the disc by outer electromagnets, after which the medium was cooled to 20–70 K. As the disc achieved superconductivity, and the state became stable, another electromagnet located under the cryostat was switched on. Due to the Meissner-Ochsenfeld effect the magnetic field lifted the disc into the air. The disc was then driven by the outer electromagnets to 5000 rpm.

A small non-conducting and non-magnetic sample was suspended over the cryostat where the rotating disc was contained. The weight of the sample was measured with high precision by an electro-optical balance system. "The sample with the initial weight of 5.47834 g was found to lose about 0.05% of its weight when placed over the levitating disc without any rotation. When the rotation speed of the disc increased, the weight of the sample became unstable and gave fluctuations from -2.5 to $+5.4$% of the initial value. [. . .] The levitating superconducting disc was found to rise by up to 7 mm when its rotation moment increased. Test measurements without the superconducting shielding disc but with all operating solenoids connected to the power supply, had no effect on the weight of the sample" [1].

Additional results were obtained by Podkletnov in 1997, with a larger disc (a $275/80\times 10$-mm toroid) run under

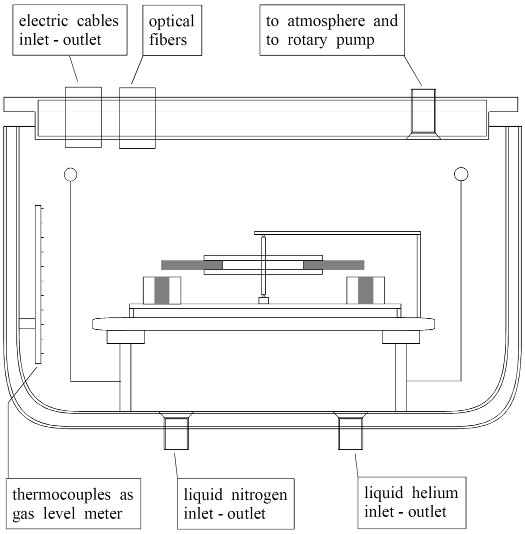

Fig. 1: Cryogenic system in Podkletnov's experiment [2]. Courtesy of E. Podkletnov. Used by permission.

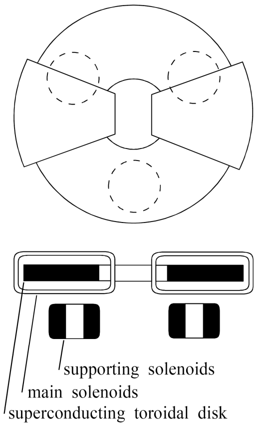

Fig. 2: Supporting and rotating solenoids in Podkletnov's experiment [2]. Courtesy of E. Podkletnov. Used by permission.

similar conditions [2]: "The levitating disc revealed a clearly measurable shielding effect against the gravitational force even without rotation. In this situation, the weight-loss values for various samples ranged from 0.05 to 0.07%. [...] Samples made from the same material and of comparable size, but with different masses, lost the same fraction of their weight. [...] Samples placed over the rotating disc initially demonstrated a weight loss of 0.3–0.5%. When the rotation speed was slowly reduced by changing the current in the solenoids, the shielding effect became considerably higher and reached 1.9–2.1% at maximum" [2].

Two groups of researchers supported by Boeing and NASA, and also a few other research teams, have attempted to replicate the Podkletnov experiment in recent years [3–7]. The main problem they encountered was the reproduction of the technology used by Podkletnov in his laboratory to produce sufficiently large superconductive ceramics. The technology is very costly: according to Podkletnov [8] this re-

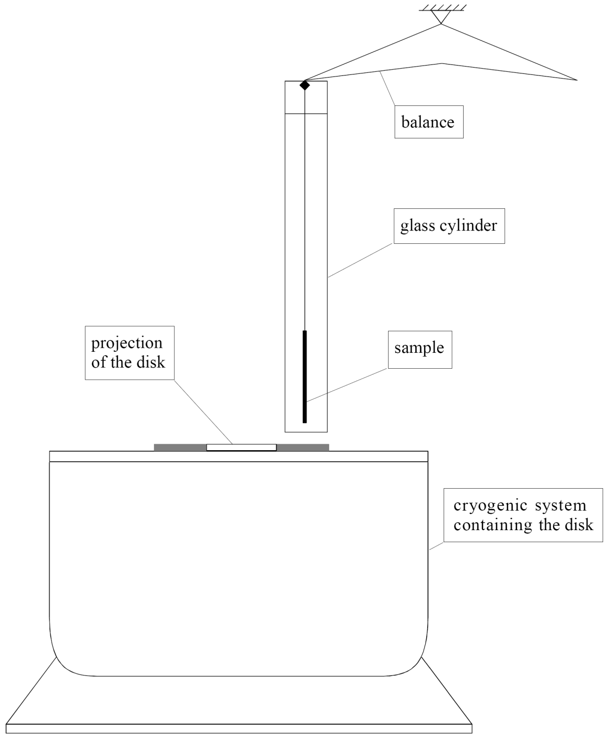

Fig. 3: Weight and pressure measurement in Podkletnov's experiment [2]. Courtesy of E. Podkletnov. Used by permission.

quires tens of millions of dollars. Therefore the aforementioned organisations tested discs of much smaller size, about 1″ diameter; so they produced controversial results at the boundary of precision measurement. As was pointed out by Podkletnov in his recent interview (April, 2006), the NASA team, after years of unsuccessful attempts, made a 12″ disc of superconductive ceramic. However, due to the crude internal structure (this is one of the main problems in making such discs), they were unable to use the disc to replicate his experiment [8].

Podkletnov also recently reported on a "gravity field generator" [8, 9] constructed in his laboratory in recent years, on the basis of the earlier observed phenomenon.

In a nutshell, the aforementioned phenomenon is as follows. We will refer to this as the *Podkletnov effect*:

> When a disc of superconductive ceramic, being in the state of superconductivity, is suspended in air by an alternating magnetic field due to an electromagnet located under the disc, the disc is the source of a radiation. This radiation, traveling like a plane wave above the disc, acts on other bodies like a negative gravity. The radiation becomes stronger with larger discs, so it depends on the disc's mass and radius. When the disc rotates uniformly, the radiation remains the same. During acceleration/braking of the disc's rotation, the radiation essentially increases.

Podkletnov claimed many times that he discovered the effect by chance, not by any theoretical prediction. Being an experimentalist who pioneered this field of research, he continued his experiments blindfolded: in the absence of a theoretical reason, the cause of the observed weight loss was unclear. This is why neither Podkletnov nor his followers at Boeing and NASA didn't develop a new experiment by which the weight loss effect substantially increased.

For instance, Podkletnov still believes that the key to his experiment is that special state which is specific to the electron gas inside superconductive materials in the state of superconductivity [8]. He and all the others therefore focused attention on low temperature superconductive ceramics, production of which, taking the large size of the discs into account, is a highly complicated and very costly process, beyond most laboratories. In fact, during the last 15 years only Podkletnov's laboratory has had the ability to produce such the discs with sufficient quality.

We propose a purely theoretical approach to this problem. We consider Podkletnov's experiment using the mathematical methods of General Relativity, in the Einstenian sense: we represent all essential components of the experiment as a result of the geometrical properties of the laboratory space such as the space non-uniformity, rotation, deformation, and curvature. We build a complete theory of the Podkletnov effect on the basis of General Relativity.

By this we will see that there is no rôle for superconductivity; Podkletnov's effect has a purely mechanical origin due in that the vertical oscillation of the disc, produced by the supporting alternating magnetic field, and the angular acceleration/braking of the disc's rotation, perturb a homogeneous field of the basic non-holonomity of the space (the basic non-othogonality of time lines to the spatial section, known from the theory of non-holonomic manifolds). As a result the non-holonomity field, initially homogeneous, is locally stressed, which is expressed by a change of the left side of Einstein's equations (geometry) and, through the conservation law, a corresponding change of the right side — the energy-momentum tensor for distributed matter (the alternating magnetic field, in this case). In other words, the perturbed field of the space non-holonomity produces energy-momentum in order to compensate for the local perturbation in itself. As we will see, the spatial momentum is directed above the disc in Podkletnov's experiment, so it works like negative gravity.

Owing to our theory we know definitely the key parameters ruling the weight loss effect. Therefore, following our calculation, it is easy to propose an experiment wherein the weight loss substantially increases.

For example, we describe a new experiment where the Podkletnov effect manifests via simple electro-mechanical equipment, without costly superconductor technology. This new experiment can be replicated in any physics laboratory.

We therefore claim thta with our mathematical theory of the Podkletnov effect, within the framework of General Relativity, we can calculate the factors ruling the weight loss. This gives us an opportunity to construct actual working devices which could revolutionize air and space travel. Such new technology, which uses high frequency electromagnetic generators and mechanical equipment instead of costly superconductors, can be the subject of further research on a commercial basis (due to the fact that applied research is outside academia).

Besides, additional energy-momentum produced by the space non-holonomity field in order to compensate for a local perturbation in itself, means that the Podkletnov effect can be used to produce new energy.

By our advanced study (not included in this paper), of our mathematical theory, that herein gives the key factors which rule the new energy, lends itself to the construction of devices which generate the new energy, powered by strong electromagnetic fields, not nuclear reactions and atomic fuel. Therefore this technology, free of radioactive waste, can be a source of clean energy.

2 The non-holonomic background space

2.1 Preliminary data from topology

In this Section we construct a space metric which includes a basic (primordial) non-holonomity, i.e. a basic field of the non-orthogonality of the time lines to the three-dimensional spatial section.

Here is some information from topology Each axis of a Euclidean space can be represented as the element of a circle with infinite radius [10]. An n-dimensional torus is the topological product of n circles. The volume of an n-dimensional torus is completely equivalent to the surface of an $(n+1)$-dimensional sphere. Any compact metric space of n dimensions can be mapped homeomorphicly into a subset of a Euclidean space of $2n+1$ dimensions.

Sequences of stochastic transitions between configurations of different dimensions can be considered as stochastic vector quantities (fields). The extremum of a distribution function for frequencies of the stochastic transitions dependent on n gives the most probable number of the dimensions, and, taking the mapping $n \rightarrow 2n+1$ into account, the most probable configuration of the space. This function was first studied in the 1960's by di Bartini [11, 12, 13]. He found that the function has extrema at $2n+1 = \pm 7$ that is equivalent to a 3-dimensional vortical torus coaxial with another, the same vortical torus, mirrored with the first one. Each of the torii is equivalent to a (3+1)-dimensional sphere. Its configuration can be easy calculated, because such formations were studied by Lewis and Larmore. A vortical torus has no breaks if the current lines coincide with the trajectory of the vortex core. Proceeding from the continuity condition, di Bartini found the most probable configuration of the vortical torus is it characterized by the ratio $E = \frac{D}{r} = \frac{1}{4}e^{6.9996968} = 274.074996$ between the torus diameter D and the radius of torus circulation r.

We apply di Bartini's result from topology to General Relativity. The time axis is represented as the element of the circle of radius $R = \frac{1}{2}D$, while the spatial axes are the elements of three small circles of radii r (the topological product of which is the 3-dimensional vortical torus). In a "metric" representation by a Minkowski diagram, the torus is a 3-dimensional spatial section of the given (3+1)-space while the time lines have some *inclination* to the the spatial section. In order for the torus (the 3-dimensional space of our world) to be uniform without break, all the time lines have the *same inclination* to the spatial section at each point of the section.

Cosines of the angles between the coordinate axes, in Riemannian geometry, are represent by the components of the fundamental metric tensor $g_{\alpha\beta}$ [14]. If the time lines are everywhere orthogonal to the spatial section, all g_{0i} are zero: $g_{0i} = 0$. Such a space is called *holonomic*. If not ($g_{0i} \neq 0$), the space is said to be *non-holonomic*. As was shown in the 1940's by Zelmanov [15, 16, 17], a field of the space non-holonomity (inclinations of the time lines to the spatial section) manifests as a rotation of the space with a 3-dimensional velocity $v_i = -\frac{c\,g_{0i}}{\sqrt{g_{00}}}$. The mathematical proof is given in Appendix 1.

So a field with the same inclination of the time lines to the spatial section is characterized, in the absence of gravitational fields, by $v_i = -c\,g_{0i} = \text{const}$ at each point of the spatial section. In other words, this is a field of the *homogeneous non-holonomity* (rotation) of the whole space. It is hard to explain such a field by everyday analogy, because it has zero angular speed, and also no centre of rotation. However owing to the space-time representation by a Minkowski diagram, it appears very simply as a field of which the time arrows pierce the hyper-surface of the spatial section with the same inclination at each point.

After di Bartini's result, we therefore conclude that the most probable configuration of the basic space (space-time) of General Relativity is represented by a primordially non-holonomic (3+1)-dimensional pseudo-Riemannian space, where the non-holonomic background field is homogeneous, which manifests in the spatial section (3-dimensional space) as the presence of two fundamental drift-fields:

1. A homogeneous field of the constant linear velocity of the background space rotation
$$\bar{v} = c\,\frac{r}{R} = \frac{2c}{E} = \text{const} = 2.187671\times10^{8}\ \text{cm/sec} \quad (1)$$
which originates from the fact that, given the non-holonomic space, the time-like spread R depends on the spatial-like spread r as $\frac{R}{r} = \frac{1}{2}E = 137.037498$. The background space rotation, with $\bar{v} = 2{,}187.671$ km/sec at each point of the space, is due to the continuity condition everywhere inside the torus;
2. A homogeneous drift-field of the constant dipole-fit linear velocity
$$\bar{\mathrm{v}} = \frac{\bar{v}}{2\pi} = \text{const} = 3.481787\times10^{7}\ \text{cm/sec} \quad (2)$$
which characterizes a spatial linear drift of the non-holonomic background relative to any given observer. The field of the spatial drift with $\bar{\mathrm{v}} = 348.1787$ km/sec is also present at each point of the space.

In the spatial section the background space rotation with $\bar{v}$=2,187.671 km/sec is observed as absolute motion. This is due to the fact that a rotation due to the space non-holonomity is relative to time, not the spatial coordinates. Despite this, as proven by Zelmanov [15, 16, 17], such a rotation relates to spatial rotation, if any.

2.2 The space metric which includes a non-holonomic background

We are going to derive the metric of a non-holonomic space, which has the aforementioned most probable configuration for the (3+1)-space of General Relativity. To do this we consider an element of volume of the space (the elementary volume).

We consider the pseudo-Riemannian (3+1)-space of General Relativity. Let it be non-holonomic so that the non-holonomity field is homogeneous, i.e. manifests as a homogeneous space-time rotation with a linear velocity v, which has the same numerical value along all three spatial axes at each point of the space. The elementary 4-dimensional interval in such a space is

$$ds^2 = c^2dt^2 + \frac{2v}{c}\,cdt\,(dx + dy + dz) - \\ - dx^2 - dy^2 - dz^2, \quad (3)$$

where the second term is not reduced, for clarity.

We denote the numerical coefficient, which characterize the space rotation (see the second term on the right side), as $\alpha = v/c$. We mean, consider the most probable configuration of the (3+1)-space, $v = \bar{v} = 2{,}187.671$ km/sec and also $\alpha = \bar{v}/c = 1/137.037498$. The ratio $\alpha = \bar{v}/c$ specific to the space (it characterizes the background non-holonomity of the space), coincides with the analytical value of Sommerfeld's fine-structure constant [11, 12, 13], connected to electromagnetic interactions.*

Given the most probable configuration of the space, each 3-dimensional volume element rotates with the linear velocity $\bar{v} = 2{,}187.671$ km/sec and moves with the velocity $\bar{\mathrm{v}} = \frac{\bar{v}}{2\pi} = 348.1787$ km/sec relative toward any observer located in the space. The metric (3) contains the space rotation only. To modify the metric for the most probable configura-

*Tests based on the quantum Hall effect and the anomalous magnetic moment of the electron, give different experimental values for Sommerfeld's constant, close to the analytical value. For instance, the latest tests (2006) gave $\alpha \simeq 1/137.035999710(96)$ [18].

$$ds^2 = c^2dt^2 + \frac{2v\,(\cos\varphi + \sin\varphi)}{c}\,cdt\,dr + \frac{2vr\,(\cos\varphi - \sin\varphi)}{c}\,cdt\,d\varphi + \frac{2v}{c}\,cdt\,dz - \\ - dr^2 + \frac{2v\mathrm{v}\,(\cos\varphi + \sin\varphi)}{c^2}\,dr\,dz - r^2d\varphi^2 + \frac{2v\mathrm{v}r\,(\cos\varphi - \sin\varphi)}{c^2}\,d\varphi\,dz - dz^2 \qquad (7)$$

tion, we should apply Lorentz' transformation along the direction of the space motion.

We choose the z-axis for the direction of space motion. For clarity of further calculation, we use the cylindrical coordinates r, φ, z

$$x = r\cos\varphi\,, \qquad y = r\sin\varphi\,, \qquad z = z\,, \qquad (4)$$

so the metric (3) in the new coordinates takes the form

$$ds^2 = c^2dt^2 + \frac{2v}{c}\,(\cos\varphi + \sin\varphi)\,cdt\,dr + \\ + \frac{2vr}{c}\,(\cos\varphi - \sin\varphi)\,cdt\,d\varphi + \frac{2v}{c}\,cdt\,dz - \\ - dr^2 - r^2d\varphi^2 - dz^2. \qquad (5)$$

Substituting the quantities $\tilde{t}$ and $\tilde{z}$ of Lorentz' transformations

$$\tilde{t} = \frac{t + \frac{\mathrm{v}z}{c^2}}{\sqrt{1-\frac{\mathrm{v}^2}{c^2}}}\,, \qquad \tilde{z} = \frac{z + \mathrm{v}t}{\sqrt{1-\frac{\mathrm{v}^2}{c^2}}}\,, \qquad (6)$$

for t and z in the metric (5), we obtain the metric for a volume element which rotates with the constant velocity $\bar{v} = \alpha c$ and approaches with the constant velocity $\mathrm{v} = \bar{\mathrm{v}}$ with respect to any observer located in the space. This is formula (7) shown on the top of this page. In that formula

$$\frac{1}{\sqrt{1-\frac{\mathrm{v}^2}{c^2}}} = \frac{1}{\sqrt{1-\frac{\bar{\mathrm{v}}^2}{c^2}}} = \text{const} \simeq 1\,, \qquad (8)$$

due to that fact that, in the framework of this problem, $\mathrm{v} \ll c$. Besides there is also $v \ll c$, so that the second order terms reduce each other. We still do not reduce the numerical coefficient c of the non-diagonal space-time terms so that they are easily recognized in the metric.

Because the non-holonomic metric (7) satisfies the most probable configuration for such a $(3+1)$-space, we regard it as the *background metric of the world*.

2.3 Study of the background metric. The main characteristics of the background space

We now calculate the main characteristics of the space which are invariant within a fixed three-dimensional spatial section, connected to an observer. Such quantities are related to the chronometric invariants, which are the physical observable quantities in General Relativity [15, 16, 17] (see Appendix 2).

After the components of the fundamental metric tensor $g_{\alpha\beta}$ are obtained from the background metric (7), we calculate the main observable characteristics of the space (see Appendix 2). It follows that in the space:

$$\frac{v}{c} = \frac{\bar{v}}{c} = \alpha = \text{const}, \qquad \frac{v\mathrm{v}}{c^2} = \frac{\alpha\bar{\mathrm{v}}}{c} = \frac{\bar{v}^2}{2\pi c^2} = \text{const}\,, \qquad (9)$$

the gravitational potential w is zero

$$g_{00} = 1\,, \qquad \mathrm{w} = c^2\big(1 - \sqrt{g_{00}}\big) = 0\,, \qquad (10)$$

the linear velocity of the space rotation $v_i = -\frac{c\,g_{0i}}{\sqrt{g_{00}}}$ is

$$\left.\begin{aligned} v_1 &= -\bar{v}\,(\cos\varphi + \sin\varphi) \\ v_2 &= -\bar{v}r\,(\cos\varphi - \sin\varphi) \\ v_3 &= -\bar{v} \end{aligned}\right\} \qquad (11)$$

the relativistic multiplier is unity (within the number of significant digits)

$$\frac{1}{\sqrt{1-\frac{\bar{\mathrm{v}}^2}{c^2}}} = \frac{1}{0.9999993} = 1\,, \qquad (12)$$

the gravitational inertial force F_i, the angular velocity of the space rotation A_{ik}, the space deformation D_{ik}, and the space curvature C_{ik} are zero

$$F_i = 0\,, \quad A_{ik} = 0\,, \quad D_{ik} = 0\,, \quad C_{ik} = 0\,, \qquad (13)$$

while of all the chr.inv.-Christoffel symbols Δ^i_{km}, only two components are non-zero,

$$\Delta^1_{22} = -r\,, \qquad \Delta^2_{12} = \frac{1}{r}\,. \qquad (14)$$

The non-holonomic background space is free of distributed matter, so the energy-momentum tensor is zero therein. Hence, as seen from the chr.inv.-Einstein equations (see Appendix 2), the background space necessarily has

$$\lambda = 0\,, \qquad (15)$$

i.e. it is also free of physical vacuum (λ-field). In other words, the non-holonomic background space is *empty*.

We conclude for the background space exposed by the non-holonomic background metric (7), that

> The non-holonomic background space satisfying the most probable configuration of the $(3+1)$-space of General Relativity is a flat pseudo-Riemannian space with the 3-dimensional Euclidean metric and a constant space-time rotation. The background space is empty; it permits neither distributed matter or vacuum (λ-field). The background space is not one an Einstein space (where $R_{\alpha\beta} = k\,g_{\alpha\beta}$, $k = \text{const}$) due to the fact that Einstein's equations have $k=0$ in the background space. To be an Einstein space, the background space should be perturbed.

Read about Einstein spaces and their formal determination in *Einstein Spaces* by A. Z. Petrov [19].

It should be noted that of the fact that the 3-dimensional Euclidean metric means only $F_i = 0$, $A_{ik} = 0$, $D_{ik} = 0$ and $C_{ik} = 0$. The Christoffel symbols can be $\Delta^i_{mn} \neq 0$ due to the curvilinear coordinates.

$$ds^2 = \left(1-\frac{2GM}{c^2z}\right)c^2dt^2 + \frac{2v\,(\cos\varphi+\sin\varphi)}{c}\,cdt\,dr + \frac{2vr\,(\cos\varphi-\sin\varphi)}{c}\,cdt\,d\varphi + \frac{2v}{c}\,cdt\,dz - \\ - dr^2 + \frac{2v\mathrm{v}\,(\cos\varphi+\sin\varphi)}{c^2}\,dr\,dz - r^2d\varphi^2 + \frac{2v\mathrm{v}r\,(\cos\varphi-\sin\varphi)}{c^2}\,d\varphi\,dz - \left(1+\frac{2GM}{c^2z}\right)dz^2 \qquad (20)$$

2.4 Perturbation of the non-holonomic background

How does a gravitational field and local rotation (the gravitational field of the Earth and the rotation of a disc, for instance) affect the metric? This we now describe.

The ratio v/c, according to the continuity condition in the space (see §2), equals Sommerfeld's fine-structure constant $\alpha = \bar{v}/c = 1/137.037498$ only if the non-holonomic background metric is *unperturbed* by a local rotation, so the space non-holonomity appears as a homogeneous field of the constant linear velocity of the space rotation $\bar{v}$, which is 2,187.671 km/sec. The gravitational potential w appears in General Relativity as $\mathrm{w} = c^2(1-\sqrt{g_{00}})$, i.e. connected to g_{00}. So the presence of a gravity field changes the linear velocity of the space rotation $v_i = -\frac{c\,g_{0i}}{\sqrt{g_{00}}}$. For an Earth-bound laboratory, we have $\frac{\mathrm{w}}{c^2} = \frac{GM}{c^2z} \simeq 7\times10^{-10}$. This numerical value is so small that perturbations of the non-holonomic background through g_{00}, by the Earth's gravitational field, are weak. Another case — local rotations. A local rotation with a linear velocity $\tilde{v}$ or a gravitational potential w perturbs the homogeneous field of the space non-holonomity, the ratio v/c in that area changes from the initial value $\alpha = \bar{v}/c = 1/137.037498$ to a new, perturbed value

$$\frac{v}{c} = \frac{\bar{v}+\tilde{v}}{c} = \alpha + \frac{\tilde{v}}{\bar{v}}\,\alpha\,. \qquad (16)$$

This fact should be taken into account in all formulae which include v or the derivatives.

Consider a high speed gyro used in aviation navigation: a 250 g rotor of 1.65″ diameter, rotating with an angular speed of 24,000 rpm. With modern equipment this is almost the uppermost speed for such a mechanically rotating system*. In such a case the background field of the space non-holonomity is perturbed near the giro as $\tilde{v} \approx 53$ m/sec, that is 2.4×10^{-5} of the background $\bar{v} = 2{,}187.671$ km/sec. Larger effects are expected for a submarine gyro, where the rotor and, hence, the linear velocity of the rotation is larger. In other words, the non-holonomic background can be substantially perturbed near such a mechanically rotating system.

2.5 The background metric perturbed by a gravitational field

The formula for the linear velocity of the space rotation

$$v_i = -c\,\frac{g_{0i}}{\sqrt{g_{00}}}\,, \qquad (17)$$

was derived by Zelmanov [15, 16, 17], due to the space non-holonomity, and originating in it. It is evident that if the same numerical value $v_i = \text{const}$ remains unchanged everywhere in the spatial section (i.e. $^*\nabla_i\, v^i = 0$)†

$$\left.\begin{aligned} v_i &= \text{const} \\ ^*\nabla_i\, v^i &= 0 \end{aligned}\right\} \qquad (18)$$

there is a *homogeneous field of the space non-holonomity*. By the formula (17), given a homogeneous field of the space non-holonomity, any local rotation of the space (expressed with g_{0i}) and also a gravitational potential (contained in g_{00}) perturb the homogeneous non-holonomic background.

We modify the background metric (7) to that case where the homogeneous non-holonomic background is perturbed by a weak gravitational field, produced by a bulky point mass M, that is usual for observations in a laboratory located on the Earth's surface or near orbit. The gravitational potential in General Relativity is $\mathrm{w} = c^2(1-\sqrt{g_{00}})$. We assume gravity acting in the z-direction, i.e. $\mathrm{w} = \frac{GM}{z}$, and we omit terms of higher than the second order in c, following the usual approximation in General Relativity (see Landau and Lifshitz [20] for instance). We substitute

$$g_{00} = \left(1-\frac{\mathrm{w}}{c^2}\right)^2 = \left(1-\frac{GM}{c^2z}\right)^2 \simeq 1-\frac{2GM}{c^2z} \neq 1 \qquad (19)$$

into the first term of the initial metric (5). After Lorentz' transformations, we obtain a formula for the non-holonomic background metric (7) perturbed by such a field of gravity. This is formula (20) displayed on the top of this page.

2.6 The background metric perturbed by a local oscillation and gravitational field

A superconducting disc in air under the influence of an alternating magnetic field of an electromagnet located beneath it, undergoes oscillatory bounces with the frequency of the current, in a vertical direction (the same that of the Earth's gravity — the z-direction in our cylindrical coordinates).

We set up a harmonic transformation of the z-coordinate

$$\tilde{z} = z + z_0\cos\frac{\Omega}{c}\,u\,, \qquad u = ct + z\,, \qquad (21)$$

where z_0 is the initial deviation (the amplitude of the oscillation), while Ω is the frequency. After calculating $d\tilde{z}$ and $d\tilde{z}^2$ (22), and using these instead of dz and dz^2 in the non-holonomic background metric (7), we obtain the background metric (7) perturbed by the local oscillation and gravitational field. This is formula (23) shown above.

*Mechanical gyros used in aviation and submarine navigation technology have rotations in the range 6,000–30,000 rpm. The upper speed is limited by problems due to friction.

†See Appendix 2 for the chr.inv.-differentiation symbol $^*\nabla$.

$$\left.\begin{aligned} d\tilde{z} &= \left(1-\frac{\Omega z_0}{c}\sin\frac{\Omega}{c}u\right)dz - \left(\frac{\Omega z_0}{c}\sin\frac{\Omega}{c}u\right)cdt \\ d\tilde{z}^2 &= \left(1-\frac{\Omega z_0}{c}\sin\frac{\Omega}{c}u\right)^2 dz^2 - \frac{2\Omega z_0}{c}\sin\frac{\Omega}{c}u\left(1-\frac{\Omega z_0}{c}\sin\frac{\Omega}{c}u\right)cdt\,dz + \left(\frac{\Omega^2 z_0^2}{c^2}\sin^2\frac{\Omega}{c}u\right)c^2dt^2 \end{aligned}\right\} \qquad (22)$$

$$\begin{aligned} ds^2 &= \left[1-\frac{2GM}{c^2\left(z+z_0\cos\frac{\Omega}{c}u\right)} - \frac{2v\Omega z_0}{c^2}\sin\frac{\Omega}{c}u - \frac{\Omega^2 z_0^2}{c^2}\sin^2\frac{\Omega}{c}u\right]c^2dt^2 + \\ &+ \frac{2v\left(\cos\varphi+\sin\varphi\right)}{c}\left(1-\frac{\Omega z_0 \mathrm{v}}{c^2}\sin\frac{\Omega}{c}u\right)cdt\,dr + \frac{2vr\left(\cos\varphi-\sin\varphi\right)}{c}\left(1-\frac{\Omega z_0\mathrm{v}}{c^2}\sin\frac{\Omega}{c}u\right)cdt\,d\varphi + \\ &+ \frac{2}{c}\left(1-\frac{\Omega z_0\mathrm{v}}{c^2}\sin\frac{\Omega}{c}u\right)\left\{v+\Omega z_0\sin\frac{\Omega}{c}u\left[1+\frac{2GM}{c^2\left(z+z_0\cos\frac{\Omega}{c}u\right)}\right]\right\}cdt\,dz - dr^2 + \\ &+ \frac{2v\mathrm{v}\left(\cos\varphi+\sin\varphi\right)}{c^2}\left(1-\frac{\Omega z_0}{c^2}\sin\frac{\Omega}{c}u\right)dr\,dz - r^2d\varphi^2 + \frac{2v\mathrm{v}r\left(\cos\varphi-\sin\varphi\right)}{c^2}\left(1-\frac{\Omega z_0}{c}\sin\frac{\Omega}{c}u\right)d\varphi\,dz - \\ &- \left[1+\frac{2GM}{c^2\left(z+z_0\cos\frac{\Omega}{c}u\right)}\right]\left(1-\frac{\Omega z_0}{c}\sin\frac{\Omega}{c}u\right)^2dz^2 \end{aligned} \qquad (23)$$

$$\begin{aligned} ds^2 &= \left(1-\frac{2GM}{c^2z}-\frac{2\Omega z_0 v}{c^2}\sin\frac{\Omega}{c}u\right)c^2dt^2 + \frac{2v\left(\cos\varphi+\sin\varphi\right)}{c}cdt\,dr + \frac{2vr\left(\cos\varphi-\sin\varphi\right)}{c}cdt\,d\varphi + \\ &+ \frac{2}{c}\left(v+\Omega z_0\sin\frac{\Omega}{c}u\right)cdt\,dz - dr^2 - r^2d\varphi^2 - dz^2 \end{aligned} \qquad (25)$$

3 The space of a suspended, vertically oscillating disc

3.1 The main characteristics of the space

Metric (23) is very difficult in use. However, under the physical conditions of a real experiment, many terms vanish so that the metric reduces to a simple form. We show how.

Consider a system like that used by Podkletnov in his experiment: a horizontally oriented disc suspended in air due to an alternating high-frequent magnetic field generated by an electromagnet located beneath the disc. Such a disc undergoes an oscillatory bounce along the vertical axis with a frequency which is the same as that of the alternating magnetic field. We apply metric (23) to this case, i.e. the metric of the space near such a disc.

First, because the initial deviation of such a disc from the rest point is very small ($z_0 \ll z$), we have

$$\frac{2GM}{c^2\left(z+z_0\cos\frac{\Omega}{c}u\right)} \simeq \frac{2GM}{c^2z}\left(1-\frac{z_0}{z}\cos\frac{\Omega}{c}u\right) \simeq \frac{2GM}{c^2z}\,. \qquad (24)$$

Second, the relativistic square is $K=1$. Third, under the conditions of a real experiment like Podkletnov's, the terms $\frac{\Omega^2 z_0^2}{c^2}$ $\frac{\Omega^2 z_0}{c}$, $\frac{\Omega z_0}{c}$, $\frac{v^2}{c^2}$ and $\frac{v}{c}$ have such small numerical values that they can be omitted from the equations. The metric (23) then takes the much simplified form, shown as expression (25) at the top of this page. In other words, the expression (25) represents the metric of the space of a disc which undergoes an oscillatory bounce orthogonal to its own plane, in the conditions of a real experiment. This is the *main metric* which will be used henceforth in our study for the Podkletnov effect.

We calculate the main observable characteristics of such a space according to Appendix 2.

In such a space the gravitational potential w and the components of the linear velocity of the space rotation v_i are

$$\mathrm{w} = \frac{GM}{z} + \left(\Omega z_0\sin\frac{\Omega}{c}u\right)v\,, \qquad (26)$$

$$\left.\begin{aligned} v_1 &= -v\left(\cos\varphi+\sin\varphi\right) \\ v_2 &= -vr\left(\cos\varphi-\sin\varphi\right) \\ v_3 &= -v-\Omega z_0\sin\frac{\Omega}{c}u \end{aligned}\right\}. \qquad (27)$$

The components of the gravitational inertial force F_i acting in such a space are

$$\left.\begin{aligned} F_1 &= \left(\Omega z_0\sin\frac{\Omega}{c}u\right)v_r + \left(\cos\varphi+\sin\varphi\right)v_t \\ F_2 &= \left(\Omega z_0\sin\frac{\Omega}{c}u\right)v_\varphi + r\left(\cos\varphi-\sin\varphi\right)v_t \\ F_3 &= \left(\Omega z_0\sin\frac{\Omega}{c}u\right)v_z - \frac{GM}{z^2} + v_t + \\ &\qquad + \Omega^2 z_0\cos\frac{\Omega}{c}u \end{aligned}\right\}, \qquad (28)$$

where the quantities v_r, v_φ, v_z, v_t denote the respective partial derivatives of v.

In such a space the components of the tensor of the angular velocities of the space rotation A_{ik} are

$$\left.\begin{aligned} A_{12} &= \frac{1}{2}\left(\cos\varphi+\sin\varphi\right)v_{\varphi}-\frac{r}{2}\left(\cos\varphi-\sin\varphi\right)v_{r} \\ A_{23} &= \frac{r}{2}\left(\cos\varphi-\sin\varphi\right)v_{z}-\frac{1}{2}\,v_{\varphi} \\ A_{13} &= \frac{1}{2}\left(\cos\varphi+\sin\varphi\right)v_{z}-\frac{1}{2}\,v_{r} \end{aligned}\right\}. \qquad (29)$$

Because we omit all quantities proportional to $\frac{v^2}{c^2}$, the chr.inv.-metric tensor $h_{ik}=-g_{ik}+\frac{1}{c^2}v_i v_k$ (the observable 3-dimensional metric tensor) becomes $h_{ik}=-g_{ik}$. Its components for the metric (25) are

$$\left.\begin{aligned} & h_{11}=1\,, \quad h_{22}=r^2, \quad h_{33}=1 \\ & h^{11}=1\,, \quad h^{22}=\frac{1}{r^2}\,, \quad h^{33}=1 \\ & h=\det\|h_{ik}\|=r^2, \qquad \frac{\partial\ln\sqrt{h}}{\partial x^1}=\frac{1}{r} \end{aligned}\right\}. \qquad (30)$$

For the tensor of the space deformation D_{ik} we obtain

$$D_{33}=D^{33}=0\,, \qquad D=h^{ik}D_{ik}=0\,. \qquad (31)$$

Among the chr.inv.-Christoffel symbols Δ^i_{km} within the framework of our approximation, only two components are non-zero,

$$\Delta^1_{22}=-r\,, \qquad \Delta^2_{12}=\frac{1}{r}\,, \qquad (32)$$

so, despite the fact that the observable curvature tensor C_{ik} which possesses all the properties of Ricci's tensor $R_{\alpha\beta}$ on the 3-dimensional spatial section (see Appendix 2) isn't zero in the space, but within the framework of our assumption it is meant to be zero: $C_{ik}=0$. In other words, although the space curvature isn't zero, it is so small that it is negligible in a real experiment such as we are considering.

These are the physical observable characteristics of a space volume element located in an Earth-bound laboratory, where the non-holonomic background of the space is perturbed by a disc which undergoes oscillatory bounces orthogonal to its own plane.

We have now obtained all the physical observable characteristics of space required by Einstein's equations. Einstein's equations describe flows of energy, momentum and matter. Using the derived equations, we will know in precisely those flows of energy and momentum near a disc which undergoes an oscillatory bounce orthogonal to its own plane. So if there is any additional energy flow or momentum flow generated by the disc, Einstein's equations show this.

3.2 Einstein's equations in the space. First conclusion about the origin of the Podkletnov effect

Einstein's equations, in terms of the physical observable quantities given in Appendix 2, were derived in the 1940's by Zelmanov [15, 16, 17] as the projections of the general covariant (4-dimensional) Einstein equations

$$R_{\alpha\beta}-\frac{1}{2}\,g_{\alpha\beta}R=-\kappa\,T_{\alpha\beta}+\lambda\,g_{\alpha\beta} \qquad (33)$$

onto the time line and spatial section of an observer.

We omit the λ-term due to its negligible effect. In considering a real situation like Podkletnov's experiment, we assume the same approximation as in the previous Section. We also take into account those physical observable characteristics of the space which are zero according to our calculation.

Einstein's equations expressed in the terms of the physical observable quantities (see Appendix 2 for the complete equations) then take the following simplified form

$$\left.\begin{aligned} & \frac{\partial F^i}{\partial x^i}-A_{ik}A^{ik}+\frac{\partial\ln\sqrt{h}}{\partial x^i}F^i=-\frac{\kappa}{2}\left(\rho c^2+U\right) \\ & \frac{\partial A^{ij}}{\partial x^j}+\frac{\partial\ln\sqrt{h}}{\partial x^j}A^{ij}=-\kappa J^i \\ & 2A_{ij}A^{\cdot j}_{k\cdot}+\frac{1}{2}\left(\frac{\partial F_i}{\partial x^k}+\frac{\partial F_k}{\partial x^i}-2\Delta^m_{ik}F_m\right)= \\ & \qquad\qquad =\frac{\kappa}{2}\left(\rho c^2-U\right)h_{ik}+\kappa U_{ik} \end{aligned}\right\} \qquad (34)$$

where $\rho=\frac{T_{00}}{g_{00}}$, $J^i=\frac{cT^i_0}{\sqrt{g_{00}}}$ and $U^{ik}=c^2T^{ik}$ are the observable projections of the energy-momentum tensor $T_{\alpha\beta}$ of distributed matter on the right side of Einstein's equations (the right side determines distributed matter which fill the space, while the left side determines the geometrical properties of the space). By their physical sense, ρ is the observable density of the energy of the matter field, J^i is the observable density of the field momentum, U^{ik} is the observable stress-tensor of the field.

In relation to Podkletnov's experiment, $T_{\alpha\beta}$ is the sum of the energy-momentum tensor of an electromagnetic field, generated by an electromagnet located beneath the disc, and also that of the other fields filling the space. We therefore attribute the energy-momentum tensor $T_{\alpha\beta}$ and its observable components ρ, J^i, U^{ik} to the common field.

Is there additional energy and momentum produced by the field of the background space non-holonomity in order to compensate for a perturbation therein, due to a disc undergoing oscillatory bounces orthogonal to its own pane? This is easy to answer using Einstein's equations, owing to the fact that given the unperturbed field of the background space non-holonomity, the linear velocity of the space rotation v isn't a function of the spatial coordinates and time $v\neq\neq f(r,\varphi,z,t)$. After F_i, A_{ik}, D_{ik}, and Δ^i_{kn} specific to the space of a suspended, vertically oscillating disc are substituted into Einstein's equations (34), the left side of the equations should contain additional terms dependent on the derivatives of v by the spatial coordinates r, φ, z, and time t. The additional terms, appearing in the left side, build

$$
\left.
\begin{aligned}
&(\cos\varphi+\sin\varphi)\,v_{tr}+(\cos\varphi-\sin\varphi)\,\frac{v_{t\varphi}}{r}+v_{tz}-(1-\cos\varphi\sin\varphi)\,v_r^2-v_z^2-\\
&-(1+\cos\varphi\sin\varphi)\,\frac{v_\varphi^2}{r^2}+\left(\cos^2\!\varphi-\sin^2\!\varphi\right)\frac{v_r v_\varphi}{r}+(\cos\varphi+\sin\varphi)\,v_r v_z+\\
&+(\cos\varphi-\sin\varphi)\,\frac{v_\varphi v_z}{r}+\frac{2GM}{z^3}+\left(\Omega z_0\sin\frac{\Omega}{c}u\right)\left(v_{rr}+\frac{v_{\varphi\varphi}}{r^2}+v_{zz}+\frac{v_r}{r}\right)=-\frac{\kappa}{2}\left(\rho c^2+U\right)\\
&\frac{(\cos\varphi-\sin\varphi)}{2r}\left(v_{r\varphi}-\frac{v_\varphi}{r}\right)-\frac{(\cos\varphi+\sin\varphi)}{2}\left(\frac{v_{\varphi\varphi}}{r^2}+v_{zz}+\frac{v_r}{r}\right)+\frac{1}{2}\,v_{rz}=\kappa J^1\\
&\frac{1}{2r^2}\left[v_{\varphi z}+(\cos\varphi+\sin\varphi)\left(v_{r\varphi}-\frac{v_\varphi}{r}\right)-r\,(\cos\varphi-\sin\varphi)\,(v_{rr}+v_{zz})\right]=\kappa J^2\\
&\frac{(\cos\varphi+\sin\varphi)}{2}\,v_{rz}+\frac{(\cos\varphi-\sin\varphi)}{2}\frac{v_{\varphi z}}{r}-\frac{1}{2}\left(v_{rr}+\frac{v_{\varphi\varphi}}{r^2}+\frac{v_r}{r}\right)=\kappa J^3\\
&(1-\cos\varphi\sin\varphi)\,v_r^2-\left(\cos^2\!\varphi-\sin^2\!\varphi\right)\frac{v_r v_\varphi}{r}+\frac{(1+2\cos\varphi\sin\varphi)}{2}\left(\frac{v_\varphi^2}{r^2}+v_z^2\right)+\\
&+\,(\cos\varphi+\sin\varphi)\,v_{tr}-(\cos\varphi+\sin\varphi)\,v_r v_z+\left(\Omega z_0\sin\frac{\Omega}{c}u\right)v_{rr}=\frac{\kappa}{2}\left(\rho c^2-U\right)+\kappa U_{11}\\
&\frac{1}{2}\Big[r\left(\cos^2\!\varphi-\sin^2\!\varphi\right)v_z^2+v_r v_\varphi-r\,(\cos\varphi-\sin\varphi)\,v_r v_z-(\cos\varphi+\sin\varphi)\,v_\varphi v_z+\\
&+(\cos\varphi+\sin\varphi)\,v_{t\varphi}+r\,(\cos\varphi-\sin\varphi)\,v_{tr}+2\left(\Omega z_0\sin\frac{\Omega}{c}u\right)\left(v_{r\varphi}-\frac{v_\varphi}{r}\right)\Big]=\kappa U_{12}\\
&\frac{1}{2}\Big[v_{tr}+(\cos\varphi+\sin\varphi)\,v_{tz}-(\cos\varphi-\sin\varphi)\,\frac{v_r v_\varphi}{r}+(1-2\cos\varphi\sin\varphi)\,v_r v_z+\\
&+(\cos\varphi+\sin\varphi)\,\frac{v_\varphi^2}{r^2}-\left(\cos^2\!\varphi-\sin^2\!\varphi\right)\frac{v_\varphi v_z}{r}+2\left(\Omega z_0\sin\frac{\Omega}{c}u\right)v_{rz}\Big]=\kappa U_{13}\\
&\frac{(1-2\cos\varphi\sin\varphi)}{2}\left(v_r^2+v_z^2\right)-\left(\cos^2\!\varphi-\sin^2\!\varphi\right)\frac{v_r v_\varphi}{r}+(1+\cos\varphi\sin\varphi)\,\frac{v_\varphi^2}{r^2}+\\
&+(\cos\varphi-\sin\varphi)\,\frac{v_{t\varphi}}{r}-(\cos\varphi-\sin\varphi)\,\frac{v_\varphi v_z}{r}+\left(\Omega z_0\sin\frac{\Omega}{c}u\right)\left(\frac{v_{\varphi\varphi}}{r^2}+\frac{v_r}{r}\right)=\frac{\kappa}{2}\left(\rho c^2-U\right)+\frac{\kappa U_{22}}{r^2}\\
&\frac{1}{2}\Big[v_{t\varphi}+r\,(\cos\varphi-\sin\varphi)\,v_{tz}+r\,(\cos\varphi-\sin\varphi)\,v_r^2-(\cos\varphi+\sin\varphi)\,v_r v_\varphi-\\
&-\,r\left(\cos^2\!\varphi-\sin^2\!\varphi\right)v_r v_z+(1+2\cos\varphi\sin\varphi)\,v_\varphi v_z+2\left(\Omega z_0\sin\frac{\Omega}{c}u\right)v_{\varphi z}\Big]=\kappa U_{23}\\
&\frac{v_r^2}{2}+v_z^2-(\cos\varphi+\sin\varphi)\,v_r v_z+\frac{v_\varphi^2}{2r^2}-(\cos\varphi-\sin\varphi)\,\frac{v_\varphi v_z}{r}+v_{tz}+\frac{2GM}{z^3}+\\
&+\left(\Omega z_0\sin\frac{\Omega}{c}u\right)v_{zz}=\frac{\kappa}{2}\left(\rho c^2-U\right)+\kappa U_{33}
\end{aligned}
\right\}
\qquad (35)
$$

respective additions to the energy and momentum of the acting electromagnetic field on the right side of the equations.

Following this line, we are looking for the energy and momentum produced by the field of the background space non-holonomity due to perturbation therein.

We substitute F_i (28), A_{ik} (29), D_{ik} (31), and Δ^i_{kn} (32), specific to the space of such an oscillating disc, into the chr.inv.-Einstein equations (34), and obtain the Einstein equations as shown in formula (35). These are actually Einstein's equations for the initial homogeneous non-holonomic space perturbed by such a disc.

As seen from the left side of the Einstein equations (35), a new energy-momentum field appears near the disc due to the appearance of a non-uniformity of the field of the background space non-holonomity (i.e. due to the functions v of the coordinates and time):

1. The field bears additional energy to the electromagnetic field energy represented in the space (see the scalar Einstein equation);
2. The field has momentum flow J^i. The momentum flow spreads from the outer space toward the disc in the r-direction, twists around the disc in the φ-direction, then rises above the disc in the z-direction (see the vectorial Einstein equations which describe the momentum flow J^1, J^2, and J^3 toward r, φ, and z-direction respectively). This purely theoretical finding explains the Podkletnov effect. According to Eugene Podkletnov, a member of his experimental team smoked a pipe a few meters away from the cryostat with the superconducting disc, during operation. By a stroke of luck, Podkletnov noticed that the tobacco smoke was attracted towards the cryostat, then twisted around it and rose above it. Podkletnov then applied a high precision balance, which immediately showed a weight loss over the cryostat. Now it is clear that the tobaccosmoke revealed the momentum flow produced by the background space non-holonomity field perturbed near the vertically oscillating disc;
3. The field has distributed stresses which are expressed by an addition to the electromagnetic field stress-tensor (see the Einstein tensor equations).

In the simplest case where Podkletnov's experiment is run in a completely holonomic space ($v=0$) the Einstein equations (35) take the simplest form

$$\left.\begin{aligned} &\frac{2GM}{z^3} = -\kappa\rho c^2 \\ &J^1 = 0\,,\quad J^2 = 0\,,\quad J^3 = 0 \\ &U_{11} = 0\,,\ U_{12} = 0\,,\ U_{13} = 0\,,\ U_{22} = 0\,,\ U_{23} = 0 \\ &\frac{2GM}{z^3} = \kappa U_{33} \end{aligned}\right\} \qquad (36)$$

This is also true in another case, where the space is non-holonomic ($v \neq 0$) but v isn't function of the spatial coordinates and time $v \neq f(r,\varphi,z,t)$, that is the unperturbed homogeneous field of the background space non-holonomity. We see that in both cases there is no additional energy and momentum flow near the disc; only the electromagnetic field flow is put into equilibrium by the Earth's gravity, directed vertically along the z-axis.

So Einstein's equations show clearly that:

> The Podkletnov effect is due to the fact that the field of the background space non-holonomity, being perturbed by a suspended, vertically oscillating disc, produces energy and momentum flow in order to compensate for the perturbation therein.

3.3 Complete geometrization of matter

Looking at the right side of the Einstein equations (35), which determine distributed matter, we see that ρ and U are included only in the scalar (first) equation and also three tensor equations with the indices 11, 22, 33 (the 5th, 8th, and 10th equations). We can therefore find a formula for U. Then, substituting the formula back into the Einstein equations for ρ and U_{11}, U_{22}, U_{33}, we can express the characteristics of distributed matter through only the physical observable characteristics of the space. This fact, coupled with the fact that the other characteristics of distributed matter (J^1, J^2, J^3, U_{12}, U_{13}, U_{13}) are expressed through only the physical observable characteristics of the space by the 2nd, 3rd, 4th, 6th, 7th, and 9th equations of the Einstein equations (35), means that considering a space in which the homogeneous non-holonomic background is perturbed by an oscillating disc, we can obtain a *complete geometrization of matter*.

Multiplying the 1st equation of (35) by the 3rd, then summing with the 5th, 8th, and 10th equations, we eliminate ρ. Then, because $U = h^{ik}U_{ik} = U_{11} + \frac{U_{22}}{r^2} + U_{33}$, we obtain a formula for U expressed only via the physical observable characteristics of the space. Substituting the obtained formula for κU into the 1st equation, we obtain a formula for ρ. After that it is easy to obtain $\rho c^2 + U$ and $\rho c^2 - U$. Using these in the three Einstein tensor equations with the diagonal indices 11, 22, 33, we obtain formulae for U_{11}, U_{22}, U_{33}, all expressed only in terms of the physical observable characteristics of the space.

The resulting equations, coupled with those of the Einstein equations (35) which determine J^1, J^2, J^3, U_{12}, U_{13}, and U_{13}, build the system of the equations (37), which completely determine the properties of distributed matter — the density of the energy ρ, the density of the momentum flow J^I, and the stress-tensor U_{ik} — only in terms of the physical observable characteristics of the space. So:

> Matter which fills the space, where a homogeneous non-holonomic background is perturbed by an oscillating disc *is completely geometrized*.

$$
\left.\begin{aligned}
&\kappa U = \frac{(1-\cos\varphi\sin\varphi)}{2}\,v_r^2 + \frac{(1+\cos\varphi\sin\varphi)}{2}\frac{v_\varphi^2}{r^2} + \frac{v_z^2}{2} - \frac{\left(\cos^2\varphi-\sin^2\varphi\right)}{2}\frac{v_r v_\varphi}{r} - \\
&- \frac{(\cos\varphi-\sin\varphi)}{2}\frac{v_\varphi v_z}{r} - \frac{(\cos\varphi+\sin\varphi)}{2}\,v_r v_z - 2\,(\cos\varphi+\sin\varphi)\,v_{tr} - \\
&- 2\,(\cos\varphi-\sin\varphi)\,\frac{v_{t\varphi}}{r} - 2\,v_{tz} - \frac{4GM}{z^3} - 2\left(\Omega z_0\sin\frac{\Omega}{c}u\right)\left(v_{rr} + \frac{v_{\varphi\varphi}}{r^2} + v_{zz} + \frac{v_r}{r}\right) \\
&\kappa\rho c^2 = \frac{3}{2}\Bigg[(1-\cos\varphi\sin\varphi)\,v_r^2 + (1+\cos\varphi\sin\varphi)\,\frac{v_\varphi^2}{r^2} + v_z^2 - \\
&- \left(\cos^2\varphi-\sin^2\varphi\right)\frac{v_r v_\varphi}{r} - (\cos\varphi-\sin\varphi)\,\frac{v_\varphi v_z}{r} - (\cos\varphi+\sin\varphi)\,v_r v_z\Bigg] \\
&\frac{\kappa}{2}\left(\rho c^2 - U\right) = \frac{(1-\cos\varphi\sin\varphi)}{2}\,v_r^2 + \frac{(1+\cos\varphi\sin\varphi)}{2}\frac{v_\varphi^2}{r^2} + \frac{v_z^2}{2} - \frac{\left(\cos^2\varphi-\sin^2\varphi\right)}{2}\frac{v_r v_\varphi}{r} - \\
&- \frac{(\cos\varphi-\sin\varphi)}{2}\frac{v_\varphi v_z}{r} - \frac{(\cos\varphi+\sin\varphi)}{2}\,v_r v_z + (\cos\varphi+\sin\varphi)\,v_{tr} + (\cos\varphi-\sin\varphi)\,\frac{v_{t\varphi}}{r} + \\
&+ v_{tz} + \frac{2GM}{z^3} + \left(\Omega z_0\sin\frac{\Omega}{c}u\right)\left(v_{rr} + \frac{v_{\varphi\varphi}}{r^2} + v_{zz} + \frac{v_r}{r}\right) \\
&\kappa J^1 = \frac{(\cos\varphi-\sin\varphi)}{2r}\left(v_{r\varphi} - \frac{v_\varphi}{r}\right) - \frac{(\cos\varphi+\sin\varphi)}{2}\left(\frac{v_{\varphi\varphi}}{r^2} + v_{zz} + \frac{v_r}{r}\right) + \frac{1}{2}\,v_{rz} \\
&\kappa J^2 = \frac{1}{2r^2}\left[v_{\varphi z} + (\cos\varphi+\sin\varphi)\left(v_{r\varphi} - \frac{v_\varphi}{r}\right) - r\,(\cos\varphi-\sin\varphi)\,(v_{rr} + v_{zz})\right] \\
&\kappa J^3 = \frac{(\cos\varphi+\sin\varphi)}{2}\,v_{rz} + \frac{(\cos\varphi-\sin\varphi)}{2}\frac{v_{\varphi z}}{r} - \frac{1}{2}\left(v_{rr} + \frac{v_{\varphi\varphi}}{r^2} + \frac{v_r}{r}\right) \\
&\kappa U_{11} = \frac{(1-\cos\varphi\sin\varphi)}{2}\,v_r^2 + (\cos\varphi\sin\varphi)\left(\frac{v_\varphi^2}{2r^2} + v_z^2\right) - \frac{\left(\cos^2\varphi-\sin^2\varphi\right)}{2}\frac{v_r v_\varphi}{r} - \frac{(\cos\varphi+\sin\varphi)}{2}\,v_r v_z + \\
&+ \frac{(\cos\varphi-\sin\varphi)}{2}\frac{v_\varphi v_z}{r} - (\cos\varphi-\sin\varphi)\,\frac{v_{t\varphi}}{r} - v_{tz} - \frac{2GM}{z^3} - \left(\Omega z_0\sin\frac{\Omega}{c}u\right)\left(\frac{v_{\varphi\varphi}}{r^2} + v_{zz} + \frac{v_r}{r}\right) \\
&\kappa U_{12} = \frac{1}{2}\Bigg[r\left(\cos^2\varphi-\sin^2\varphi\right)v_z^2 + v_r v_\varphi - r\,(\cos\varphi-\sin\varphi)\,v_r v_z - (\cos\varphi+\sin\varphi)\,v_\varphi v_z + \\
&+ (\cos\varphi+\sin\varphi)\,v_{t\varphi} + r\,(\cos\varphi-\sin\varphi)\,v_{tr} + 2\left(\Omega z_0\sin\frac{\Omega}{c}u\right)\left(v_{r\varphi} - \frac{v_\varphi}{r}\right)\Bigg] \\
&\kappa U_{13} = \frac{1}{2}\Bigg[v_{tr} + (\cos\varphi+\sin\varphi)\,v_{tz} - (\cos\varphi-\sin\varphi)\,\frac{v_r v_\varphi}{r} + (1-2\cos\varphi\sin\varphi)\,v_r v_z + \\
&+ (\cos\varphi+\sin\varphi)\,\frac{v_\varphi^2}{r^2} - \left(\cos^2\varphi-\sin^2\varphi\right)\frac{v_\varphi v_z}{r} + 2\left(\Omega z_0\sin\frac{\Omega}{c}u\right)v_{rz}\Bigg] \\
&\frac{\kappa U_{22}}{r^2} = -(\cos\varphi\sin\varphi)\left(\frac{v_r^2}{2} + v_z^2\right) + \frac{(1+\cos\varphi\sin\varphi)}{2}\frac{v_\varphi^2}{r^2} - \frac{\left(\cos^2\varphi-\sin^2\varphi\right)}{2}\frac{v_r v_\varphi}{r} - \\
&- \frac{(\cos\varphi-\sin\varphi)}{2}\frac{v_\varphi v_z}{r} + \frac{(\cos\varphi+\sin\varphi)}{2}\,v_r v_z - (\cos\varphi+\sin\varphi)\,v_{tr} - v_{tz} - \frac{2GM}{z^3} - \left(\Omega z_0\sin\frac{\Omega}{c}u\right)(v_{rr} + v_{zz}) \\
&\kappa U_{23} = \frac{1}{2}\Bigg[v_{t\varphi} + r\,(\cos\varphi-\sin\varphi)\,v_{tz} + r\,(\cos\varphi-\sin\varphi)\,v_r^2 - (\cos\varphi+\sin\varphi)\,v_r v_\varphi - \\
&- r\left(\cos^2\varphi-\sin^2\varphi\right)v_r v_z + (1+2\cos\varphi\sin\varphi)\,v_\varphi v_z + 2\left(\Omega z_0\sin\frac{\Omega}{c}u\right)v_{\varphi z}\Bigg] \\
&\kappa U_{33} = \frac{(\cos\varphi\sin\varphi)}{2}\left(v_r^2 - \frac{v_\varphi^2}{r^2}\right) + \frac{v_z^2}{2} - \frac{(\cos\varphi+\sin\varphi)}{2}\,v_r v_z + \frac{\left(\cos^2\varphi-\sin^2\varphi\right)}{2}\frac{v_r v_\varphi}{r} - \\
&- \frac{(\cos\varphi-\sin\varphi)}{2}\frac{v_\varphi v_z}{r} - (\cos\varphi+\sin\varphi)\,v_{tr} - (\cos\varphi-\sin\varphi)\,\frac{v_{t\varphi}}{r} - \left(\Omega z_0\sin\frac{\Omega}{c}u\right)\left(v_{rr} + \frac{v_{\varphi\varphi}}{r^2} + \frac{v_r}{r}\right)
\end{aligned}\right\}\qquad (37)
$$

There is just one question still to be answered. What is the nature of the matter?

Among the matter different from the gravitational field, only the isotropic electromagnetic field was previously geometrized — that for which the metric is determined by the Rainich condition [23, 24, 25]

$$R=0\,,\qquad R_{\alpha\rho}R^{\rho\beta}=\frac{1}{4}\,\delta^{\beta}_{\alpha}\left(R_{\rho\sigma}R^{\rho\sigma}\right)=0 \tag{38}$$

and the Nordtvedt-Pagels condition [26]

$$\eta_{\mu\varepsilon\gamma\sigma}\left(R^{\delta\gamma;\sigma}R^{\varepsilon\tau}-R^{\delta\varepsilon;\sigma}R^{\gamma\tau}\right)=0\,. \tag{39}$$

The Rainich condition and the Nordtvedt-Pagels condition, being applied to the left side of Einstein's equations, completely determine the properties of the isotropic electromagnetic field on the right side. In other words, the aforementioned conditions determine both the geometric properties of the space and the properties of a pervading isotropic electromagnetic field.

An isotropic electromagnetic field is such where the field invariants $F_{\alpha\beta}F^{\alpha\beta}$ and $F_{*\alpha\beta}F^{\alpha\beta}$, constructed from the electromagnetic field tensor $F_{\alpha\beta}$ and the field pseudo-tensor $F^{*\alpha\beta}=\frac{1}{2}\,\eta^{\alpha\beta\mu\nu}F_{\mu\nu}$ dual, are zero

$$F_{\alpha\beta}F^{\alpha\beta}=0\,,\qquad F_{*\alpha\beta}F^{\alpha\beta}=0\,, \tag{40}$$

so the isotropic electromagnetic field has a structure truncated to that of an electromagnetic field in general.

In our case we have no limitation on the structure of the electromagnetic field, so we use the energy-momentum tensor of the electromagnetic field in the general form [20]

$$T_{\alpha\beta}=\frac{1}{4\pi}\left(-F_{\alpha\sigma}F_{\beta\cdot}^{\cdot\sigma}+\frac{1}{4}\,F_{\mu\nu}F^{\mu\nu}g_{\alpha\beta}\right), \tag{41}$$

whence the observable density of the field energy $\rho=\frac{T_{00}}{g_{00}}$ and the trace $U=h^{ik}U_{ik}$ of the observable stress-tensor of the field $U^{ik}=c^2T^{ik}$ are connected by the relation

$$\rho c^2=U\,. \tag{42}$$

In other words, if besides the gravitational field there is be only an electromagnetic field, we should have $\rho c^2=U$ for distributed matter in the Einstein equations.

However, as seen in the 2nd equation of the system (37), $\rho c^2-U\neq 0$ in the Einstein equations, for the only reason that, in the case we are considering, the laboratory space is filled not only by the Earth's gravitational field and an alternating magnetic field which supports the disc in air, but also another field appeared due to the fact that the oscillating disc perturbs the non-holonomic background of the space. The perturbation field, as shown in the previous Section, bears energy and momentum*, so it can be taken as a field of distributed matter. In other words,

> We have obtained a complete geometrization of matter consisting of an arbitrary electromagnetic field and a perturbation field of the non-holonomic background of the space.

3.4 The conservation law

When considering the geodesic equations in a space, the hon-holonomic background of which is perturbed by a disc undergoing oscillatory bounces orthogonal to its own plane, we need to know the space distribution of the perturbation, i.e. some relations between the functions $v_t=\frac{\partial v}{\partial t}$, $v_r=\frac{\partial v}{\partial r}$, $v_\varphi=\frac{\partial v}{\partial \varphi}$, $v_z=\frac{\partial v}{\partial z}$, which are respective partial derivatives of the value v of the linear velocity of the space rotation v_i.

The functions v_t, v_r, v_φ, v_z are contained in the left side (geometry) of the Einstein equations we have obtained. Therefore, from a formal point of view, to find the functions we should integrate the Einstein equations. However the Einstein equations are represented in a non-empty space, so the right side of the equations is not zero, but occupied by the energy-momentum tensor $T_{\alpha\beta}$ of distributed matter which fill the space. Hence, to obtain the functions v_t, v_r, v_φ, v_z from the Einstein equations, we should express the right side of the equations — the energy-momentum tensor of distributed matter $T_{\alpha\beta}$ — through the functions as well.

Besides, in our case, $T_{\alpha\beta}$ represents not only the energy-momentum of the electromagnetic field but also the energy-momentum produced by the field of the background space non-holonomity compensating the perturbation therein. Yet we cannot divide one energy-momentum tensor by another. So we must consider the energy-momentum tensor for the common field, which presents a problem, because we have no formulae for the components of the energy-momentum tensor of the common field. In other words, we are enforced to operate with the components of $T_{\alpha\beta}$ as merely some quantities ρ, J^i, and U^{ik}.

How to express $T_{\alpha\beta}$ through the functions v_t, v_r, v_φ, v_z, aside for by the Einstein equations? In another case we would be led to a dead end. However, our case of distributed matter is completely geometrized. In other words, the geometrical structure of the space and the space distribution of the energy-momentum tensor $T_{\alpha\beta}$ are the same things. We can therefore find the functions v_t, v_r, v_φ, v_z from the space distribution of $T_{\alpha\beta}$, via the equations of the conservation law

$$\nabla_\sigma T^{\alpha\sigma}=0\,. \tag{43}$$

The conservation law in the chr.inv.-form, i.e. represented as the projections of equation (43) onto the time line and spatial section of an observer, is [15]

$$\left.\begin{aligned}
&\frac{{}^*\partial\rho}{\partial t}+D\rho+\frac{1}{c^2}D_{ij}U^{ij}+\left({}^*\nabla_i-\frac{1}{c^2}F_i\right)J^i-\frac{1}{c^2}F_iJ^i=0\\
&\frac{{}^*\partial J^k}{\partial t}+2\left(D^k_i+A_{i\cdot}^{\cdot k}\right)J^i+\left({}^*\nabla_i-\frac{1}{c^2}F_i\right)U^{ik}-\rho F^k=0
\end{aligned}\right\} \tag{44}$$

*The fact that the space non-holonomity field bears energy and momentum was first shown in the earlier publication [27], where the field of a reference body was considered.

$$\left.\begin{aligned}
&\frac{\partial\rho}{\partial t}+\frac{\partial J^1}{\partial r}+\frac{\partial J^2}{\partial\varphi}+\frac{\partial J^3}{\partial z}+\frac{1}{r}\,J^1=0\\
&\frac{\partial J^1}{\partial t}-\big[(\cos\varphi+\sin\varphi)\,v_\varphi-r\,(\cos\varphi-\sin\varphi)\,v_r\big]\,J^2-\big[(\cos\varphi+\sin\varphi)\,v_z-v_r\big]\,J^3+\\
&+\frac{\partial U_{11}}{\partial r}+\frac{1}{r^2}\frac{\partial U_{12}}{\partial\varphi}+\frac{\partial U_{13}}{\partial z}+\frac{1}{r}\left(U_{11}-\frac{U_{22}}{r^2}\right)-\rho\left[\left(\Omega z_0\sin\frac{\Omega}{c}\,u\right)v_r+(\cos\varphi+\sin\varphi)\,v_t\right]=0\\
&\frac{\partial J^2}{\partial t}-\left[(\cos\varphi+\sin\varphi)\,\frac{v_\varphi}{r^2}-(\cos\varphi-\sin\varphi)\,\frac{v_r}{r}\right]J^1-\left[(\cos\varphi-\sin\varphi)\,\frac{v_z}{r}-\frac{v_\varphi}{r^2}\right]J^3+\\
&+\frac{\partial}{\partial r}\left(\frac{U_{12}}{r^2}\right)+\frac{1}{r^2}\left(\frac{1}{r^2}\frac{\partial U_{22}}{\partial\varphi}+\frac{\partial U_{23}}{\partial z}+\frac{3}{r}\,U_{12}\right)-\rho\left[\left(\Omega z_0\sin\frac{\Omega}{c}\,u\right)\frac{v_\varphi}{r^2}+\frac{(\cos\varphi-\sin\varphi)}{r}\,v_t\right]=0\\
&\frac{\partial J^3}{\partial t}+\big[(\cos\varphi+\sin\varphi)\,v_z-v_r\big]\,J^1+\big[r\,(\cos\varphi-\sin\varphi)\,v_z-v_\varphi\big]\,J^2+\\
&+\frac{\partial U_{13}}{\partial r}+\frac{1}{r^2}\frac{\partial U_{23}}{\partial\varphi}+\frac{\partial U_{33}}{\partial z}+\frac{1}{r}\,U_{13}-\rho\left[\left(\Omega z_0\sin\frac{\Omega}{c}\,u\right)v_z-\frac{GM}{z^2}+v_t+\Omega^2 z_0\cos\frac{\Omega}{c}\,u\right]=0
\end{aligned}\right\}\qquad(46)$$

where $\rho=\frac{T_{00}}{g_{00}}$, $J^i=\frac{cT_0^i}{\sqrt{g_{00}}}$ and $U^{ik}=c^2T^{ik}$ are the observable projections of the energy-momentum tensor $T_{\alpha\beta}$ of distributed matter. The chr.inv.-conservation equations, taking our assumptions for real experiment into account, take the simplified form

$$\left.\begin{aligned}
&\frac{\partial\rho}{\partial t}+\frac{\partial J^i}{\partial x^i}+\frac{\partial\ln\sqrt{h}}{\partial x^i}\,J^i=0\\
&\frac{\partial J^k}{\partial t}+2A_{i\cdot}^{\cdot k}J^i+\frac{\partial U^{ik}}{\partial x^i}+\frac{\partial\ln\sqrt{h}}{\partial x^i}\,U^{ik}+\\
&\qquad+\Delta^k_{im}U^{im}-\rho F^k=0
\end{aligned}\right\}.\qquad(45)$$

Substituting into the equations the formulae for D, D^k_i, $A_{i\cdot}^{\cdot k}$, $\frac{\partial\ln\sqrt{h}}{\partial x^i}$, Δ^k_{im}, and F^k, we obtain a system of the conservation equations (46) wherein we should substitute ρ, J^i, and U^{ik} from the Einstein equations (37) then, reducing similar terms, arrive at some relations between the functions v_t, v_r, v_φ, v_z. The Einstein equations (37) substituted into (46) evidently result in intractable equations. It seems that we will have no chance of solving the resulting equations without some simplification according to real experiment. We should therefore take the simplification into account from the beginning.

First, the scalar equation of the conservation law (44) under the conditions of a real experiment takes the form of (45), which in another notation is

$$\frac{\partial\rho}{\partial t}+{}^*\nabla_i\,J^i=0\,.\qquad(47)$$

The 2nd equation of (37) determines ρ: the quantity is $\rho\sim\frac{1}{c^2}$. Omitting the term proportional to $\frac{1}{c^2}$ as its effect is negligible in a real experiment, we obtain the scalar equation of the conservation law in the form*

$${}^*\nabla_i\,J^i=0\,,\qquad(48)$$

i.e. the chr.inv.-derivative of the common flow of the spatial momentum of distributed matter is zero to within the approximation of a first-order experiment. This finding has a very important meaning:

> Given a space, the non-holonomic background of which is perturbed by an oscillating disc, the common flow of the momentum of distributed matter on the spatial section of such a space is conserved in a first-order experiment.

Second, there are three states of the disc in Podkletnov's experiment: (1) uniform rotation; (2) non-uniform rotation (acceleration/deceleration); (3) non-rotating disc. To study the case of a rotating disc we should introduce, into the metric (25), additional terms which take the rotation into account. We don't do this now, for two reasons: (1) the additional terms introduced into the metric (25) make the equations of the theory too complicated; (2) the case of a non-rotating disc is that main case where, according Podkletnov's experiments, the weight-loss effect appears in the basic form; accelerating/decelerating rotation of the disc produces only additions to the basic weight-loss. So, to understand the origin of the weight-loss phenomenon it is most reasonable to first consider perturbation of the background field of the space non-holonomity by a non-rotating disc. Because such a disc lies horizontally in the plane $r\varphi$ (horizontal plane), we should assume $v_z=0$, while the fact that there $v_r\neq 0$ and $v_\varphi\neq 0$ means freedom for oscillation in the plane $r\varphi$ (accelerating or decelerating twists in the plane) as a result of vertical oscillation of such a disc (otherwise, for no oscillation in the plane $r\varphi$, the conservation equations would become zero). The fact that $\varphi\neq\text{const}$ in the equations means the same.

As a result, the conservation equations (46), with the aforementioned assumptions taken into account, take the form (49). The characteristics of distributed matter such as the momentum flow J^i and the stress-tensor U^{ik}, resulting from

*The chr.inv.-differential operators are completely determined, according to [15, 16], in Appendix 2.

$$\left.\begin{aligned}
&\frac{\partial J^1}{\partial t}-\big[(\cos\varphi+\sin\varphi)\,v_\varphi-r\,(\cos\varphi-\sin\varphi)\,v_r\big]\,J^2+v_r\,J^3+\frac{\partial U_{11}}{\partial r}+\frac{1}{r^2}\frac{\partial U_{12}}{\partial\varphi}+\frac{1}{r}\left(U_{11}-\frac{U_{22}}{r^2}\right)=0\\
&\frac{\partial J^2}{\partial t}-\left[(\cos\varphi+\sin\varphi)\,\frac{v_\varphi}{r^2}-(\cos\varphi-\sin\varphi)\,\frac{v_r}{r}\right]J^1+\frac{v_\varphi}{r^2}\,J^3+\frac{\partial}{\partial r}\left(\frac{U_{12}}{r^2}\right)+\frac{1}{r^2}\left(\frac{1}{r^2}\frac{\partial U_{22}}{\partial\varphi}+\frac{3}{r}\,U_{12}\right)=0\\
&\frac{\partial J^3}{\partial t}-v_r\,J^1-v_\varphi\,J^2+\frac{\partial U_{13}}{\partial r}+\frac{1}{r^2}\frac{\partial U_{23}}{\partial\varphi}+\frac{1}{r}\,U_{13}=0
\end{aligned}\right\}\qquad(49)$$

$$\left.\begin{aligned}
&\kappa J^1=\frac{(\cos\varphi-\sin\varphi)}{2r}\left(v_{r\varphi}-\frac{v_\varphi}{r}\right)-\frac{(\cos\varphi+\sin\varphi)}{2}\left(\frac{v_{\varphi\varphi}}{r^2}+\frac{v_r}{r}\right)\\
&\kappa J^2=\frac{1}{2r^2}\left[(\cos\varphi+\sin\varphi)\left(v_{r\varphi}-\frac{v_\varphi}{r}\right)-r\,(\cos\varphi-\sin\varphi)\;v_{rr}\right]\\
&\kappa J^3=-\frac{1}{2}\left(v_{rr}+\frac{v_{\varphi\varphi}}{r^2}+\frac{v_r}{r}\right)\\
&\kappa U_{11}=\frac{(\cos\varphi-\sin\varphi)}{2}\,v_r^2+(\cos\varphi\sin\varphi)\,\frac{v_\varphi^2}{2r^2}-\frac{\left(\cos^2\varphi-\sin^2\varphi\right)}{2}\,\frac{v_rv_\varphi}{r}-(\cos\varphi-\sin\varphi)\,\frac{v_{t\varphi}}{r}-\\
&\quad-\frac{2GM}{z^3}-\left(\Omega z_0\sin\frac{\Omega}{c}\,u\right)\left(\frac{v_{\varphi\varphi}}{r^2}+\frac{v_r}{r}\right)\\
&\kappa U_{12}=\frac{1}{2}\left[v_rv_\varphi+(\cos\varphi+\sin\varphi)\,v_{t\varphi}+r\,(\cos\varphi-\sin\varphi)\,v_{tr}+2\left(\Omega z_0\sin\frac{\Omega}{c}\,u\right)\left(v_{r\varphi}-\frac{v_\varphi}{r}\right)\right]\\
&\kappa U_{13}=\frac{1}{2}\left[v_{tr}-(\cos\varphi-\sin\varphi)\,\frac{v_rv_\varphi}{r}+(\cos\varphi+\sin\varphi)\,\frac{v_\varphi^2}{r^2}\right]\\
&\frac{\kappa U_{22}}{r^2}=-(\cos\varphi\sin\varphi)\,\frac{v_r^2}{2}+\frac{(\cos\varphi+\sin\varphi)}{2}\frac{v_\varphi^2}{r^2}-\frac{\left(\cos^2\varphi-\sin^2\varphi\right)}{2}\,\frac{v_rv_\varphi}{r}-(\cos\varphi+\sin\varphi)\,v_{tr}-\\
&\quad-\frac{2GM}{z^3}-\left(\Omega z_0\sin\frac{\Omega}{c}\,u\right)v_{rr}\\
&\kappa U_{23}=\frac{1}{2}\left[v_{t\varphi}+r\,(\cos\varphi-\sin\varphi)\,v_r^2-(\cos\varphi+\sin\varphi)\,v_rv_\varphi\right]\\
&\kappa U_{33}=\frac{\cos\varphi\sin\varphi}{2}\left(v_r^2-\frac{v_\varphi^2}{r^2}\right)+\frac{\left(\cos^2\varphi-\sin^2\varphi\right)}{2}\,\frac{v_rv_\varphi}{r}-(\cos\varphi+\sin\varphi)\,v_{tr}-(\cos\varphi-\sin\varphi)\,\frac{v_{t\varphi}}{r}-\\
&\quad-\left(\Omega z_0\sin\frac{\Omega}{c}\,u\right)\left(v_{rr}+\frac{v_{\varphi\varphi}}{r^2}+\frac{v_r}{r}\right)
\end{aligned}\right\}\qquad(50)$$

the Einstein equations (37), were collected in complete form into the system (37). Under the aforementioned assumptions they take the form (50).

We substitute the respective components of J^i and U^{ik} (50) into the conservation equations (49). After algebra, reducing similar terms, the first two equations of (49) become identically zero, while the third equation takes the form:

$$v_r=\frac{v_\varphi}{r}\,,\qquad(51)$$

The solution $v_r=\frac{v_\varphi}{r}$ we have obtained from the conservation equations satisfies by the function

$$v=B(t)\,r\,e^{\varphi},\qquad(52)$$

where $B(t)$ is a function of time t. Specific formula for the function $B(t)$ should be determined by nature of the phenomenon or the conditions of the experiment.

The solution indicates a dependency between the distributions of v in the r-direction and φ-direction in the space, if the non-holonomic background is perturbed by a disc lying in the $r\varphi$ plane and oscillating in the z-direction.

In other words, the conservation equations in common with the Einstein equations we have obtained mean that:

> A disc, oscillating orthogonally to its own plane, perturbs the field of the background non-holonomity of the space. Such a motion of a disc places a limitation on the geometric structure of the space. The limitation is manifested as a specific distribution of the linear velocity of the space rotation. This distribution means that such a disc should also have small twists in its own plane due to the perturbed non-holonomic background.

$$\left.\begin{aligned} &\ddot{r} - \big[(\cos\varphi+\sin\varphi)\,v_\varphi - r\,(\cos\varphi-\sin\varphi)\,v_r\big]\,\dot{\varphi} - \big[(\cos\varphi+\sin\varphi)\,v_z - v_r\big]\,\dot{z} - \\ &- (\cos\varphi+\sin\varphi)\,v_t - r\dot{\varphi}^2 - \left(\Omega z_0 \sin\frac{\Omega}{c}u\right) v_r = 0 \\ &\ddot{\varphi} + \left[(\cos\varphi+\sin\varphi)\,\frac{v_\varphi}{r^2} - (\cos\varphi-\sin\varphi)\,\frac{v_r}{r}\right]\dot{r} - \left[(\cos\varphi-\sin\varphi)\,\frac{v_z}{r} - \frac{v_\varphi}{r^2}\right]\dot{z} - \\ &- (\cos\varphi-\sin\varphi)\,\frac{v_t}{r} + \frac{2\dot{r}}{r}\,\dot{\varphi} - \left(\Omega z_0 \sin\frac{\Omega}{c}u\right)\frac{v_\varphi}{r^2} = 0 \\ &\ddot{z} + \big[(\cos\varphi+\sin\varphi)\,v_z - v_r\big]\,\dot{r} + \big[r\,(\cos\varphi-\sin\varphi)\,v_z - v_\varphi\big]\,\dot{\varphi} - \\ &+ \frac{GM}{z^2} - v_t - \left(\Omega z_0 \sin\frac{\Omega}{c}u\right) v_z - \Omega^2 z_0 \cos\frac{\Omega}{c}u = 0 \end{aligned}\right\} \qquad (60)$$

3.5 The geodesic equations in the space. Final conclusion about the forces driving the Podkletnov effect

This is the final part of our mathematical theory of the Podkletnov effect. Here, using the Einstein equations and the equations of the conservation law we have developed, we deduce an additional force that produces the weight-loss effect in Podkletnov's experiment, i.e. the weight-loss over a superconducting disc which is supported in air by an alternating magnetic field.

As is well known, motion in a gravitational field of a free test-particle of rest-mass m_0 is described by the equations of geodesic lines (the geodesic equations). The geodesic equations are, from a purely mathematical viewpoint, the equations of parallel transfer of the four-dimensional vector of the particle's momentum $P^\alpha = m_0\frac{dx^\alpha}{ds}$ along the particle's 4-dimensional trajectory

$$\frac{dP^\alpha}{ds} + \Gamma^\alpha_{\mu\nu} P^\mu \frac{dx^\nu}{ds} = 0\,, \qquad (53)$$

where $\Gamma^\alpha_{\mu\nu}$ are Christoffel's symbols of the 2nd kind, while ds is the 4-dimensional interval along the trajectory.

The geodesic equations (53), being projected onto the time line and spatial section of an observer, and expressed through the physical observable characteristics of a real laboratory space of a real observer, are known as the chr.inv.-geodesic equations. They were deduced in 1944 by Zelmanov [15, 16]. The related scalar equation is the projection onto the time line of the observer, while the 3-dimensional vector equation is the projection onto his spatial section, and manifests the 3rd Newtonian law for the test-particle:

$$\left.\begin{aligned} &\frac{dm}{d\tau} - \frac{m}{c^2}F_i \mathrm{v}^i + \frac{m}{c^2}D_{ik}\mathrm{v}^i\mathrm{v}^k = 0 \\ &\frac{d(m\mathrm{v}^i)}{d\tau} + 2m\left(D^i_k + A^{\cdot i}_{k\cdot}\right)\mathrm{v}^k - mF^i + m\Delta^i_{nk}\mathrm{v}^n\mathrm{v}^k = 0 \end{aligned}\right\} \qquad (54)$$

where m is the relativistic mass of the particle, v^i is the 3-dimensional observable velocity of the particle, and τ is the physical observable or proper time* [15, 16]

$$m = \frac{m_0}{\sqrt{1-\mathrm{v}^2/c^2}}\,, \qquad \mathrm{v}^i = \frac{dx^i}{d\tau}\,, \qquad (55)$$

$$d\tau = \sqrt{g_{00}}\,dt + \frac{g_{0i}}{c\sqrt{g_{00}}}\,dx^i = \sqrt{g_{00}}\,dt - \frac{1}{c^2}\,v_i dx^i. \qquad (56)$$

With the simplifications for the real experiment we are considering, the chr.inv.-geodesic equations (54) take the form

$$\left.\begin{aligned} &\frac{dm}{d\tau} = 0 \\ &\frac{d(m\mathrm{v}^i)}{d\tau} + 2mA^{\cdot i}_{k\cdot}\mathrm{v}^k - mF^i + m\Delta^i_{nk}\mathrm{v}^n\mathrm{v}^k = 0 \end{aligned}\right\} \qquad (57)$$

that is, in component notation,

$$\left.\begin{aligned} &\frac{dm}{d\tau} = 0 \\ &\frac{d}{d\tau}\left(m\frac{d\mathrm{v}^1}{d\tau}\right) + 2mA^{\cdot 1}_{k\cdot}\mathrm{v}^k - mF^1 + m\Delta^1_{22}\mathrm{v}^2\mathrm{v}^2 = 0 \\ &\frac{d}{d\tau}\left(m\frac{d\mathrm{v}^2}{d\tau}\right) + 2mA^{\cdot 2}_{k\cdot}\mathrm{v}^k - mF^2 + 2m\Delta^2_{12}\mathrm{v}^1\mathrm{v}^2 = 0 \\ &\frac{d}{d\tau}\left(m\frac{d\mathrm{v}^3}{d\tau}\right) + 2mA^{\cdot 3}_{k\cdot}\mathrm{v}^k - mF^3 = 0 \end{aligned}\right\} \qquad (58)$$

which are actual chr.inv.-equations of motion of a free test-body in the space, whose non-holonomic homogeneous background is perturbed by an oscillating disc.

The scalar geodesic equation of (58) says

$$m = \text{const}\,, \qquad (59)$$

so taking this fact into account and introducing the notation $\mathrm{v}^1 = \frac{dr}{d\tau} = \dot{r}$, $\mathrm{v}^2 = \frac{d\varphi}{d\tau} = \dot{\varphi}$, $\mathrm{v}^3 = \frac{dz}{d\tau} = \dot{z}$, we obtain a system of three vector equations of motion of the test-body (60), wherein $v_t = \frac{\partial v}{\partial t}$, $v_r = \frac{\partial v}{\partial r}$, $v_\varphi = \frac{\partial v}{\partial \varphi}$, $v_z = \frac{\partial v}{\partial z}$.

*This is that real time which is registered by the observer in his real laboratory space. Intervals of the physical observable time $d\tau$ and the observable spatial coordinates dx^i are determined, by the theory of physical observable quantities (chronometric invariants) as the projections of the interval of the 4-dimensional coordinates dx^α onto the time line and spatial section of an observer, i.e.: $b_\alpha dx^\alpha = c d\tau$, $h^i_\alpha dx^\alpha = dx^i$ [15, 16]. See Appendix 2 for the details of such a projection.

Because the terms containing z_0 in equations (60) are very small, they can be considered to be small harmonic corrections. Such equations can always be solved using the small parameter method of Poincaré. The Poincaré method is also known as the perturbation method, because we consider the right side as a perturbation of a harmonic oscillation described by the left side. The Poincaré method is related to exact solution methods, because a solution produced with the method is a power series expanded by a small parameter (see Lefschetz, Chapter XII, §2 of [21]).

However our task is much simpler. We are looking for an approximate solution of the system of the vector equations of motion in order to see the main forces acting in the basic Podkletnov experiment. We therefore simplify the equations as possible. First we take into account that, in the condition of Podkletnov's experiment, the suspended test-body has freedom to move only in the z-direction (i.e. up or down in a vertical direction, which is the direction of the acting force of gravity). In other words, concerning a free test-body falling from above the disc, we take $\dot{r}=0$ and $\dot{\varphi}=0$ despite the forces $\ddot{r}$ and $\ddot{\varphi}$ acting it in the r-direction and the φ-direction are non-zero. Second, rotational oscillation of the disc in the $r\varphi$–plane is very small. We therefore regard φ as a small quantity, so $\sin\varphi\simeq\varphi$ and $\cos\varphi\simeq 1$. Third, by the conservation equations, $v_\varphi = r\,v_r$.

Taking all the assumptions into account, the equations of motion (60) take the much simplified form

$$\left.\begin{aligned} &\ddot{r}+v_r\dot{z}-(1+\varphi)\,v_t-\left(\Omega z_0\sin\frac{\Omega}{c}u\right)v_r=0\\ &\ddot{\varphi}+\frac{v_r}{r}\,\dot{z}-(1-\varphi)\,v_t-\left(\Omega z_0\sin\frac{\Omega}{c}u\right)\frac{v_r}{r}=0\\ &\ddot{z}+g-v_t-\Omega^2 z_0\cos\frac{\Omega}{c}u=0 \end{aligned}\right\} \tag{61}$$

where $g=\frac{GM}{z^2}$ is the acceleration produced by the Earth's force of gravity, remaining constant for the experiment.

For Podkletnov's experiment, $v_t=\text{const}$, and this value depends on the specific parameters of the vertically oscillating disc, such as its diameter, the frequency and amplitude of its vibration. The harmonic term in the third equation is a small correction which can only shake a test-body in the z-direction; this term cannot be a source of a force acting in just one direction. Besides, the harmonic term has a very small numerical value, and so it can be neglected. In such a case, the third equation of motion takes the simple form

$$\ddot{z}+g-v_t=0\,, \tag{62}$$

where the last term is a correction to the acting force of gravity due to the perturbed field of the background space non-holonomity.

Integrating the equation $\ddot{z}=-g+v_t$, we obtain

$$z=-\frac{g-v_t}{2}\,\tau^2+C_1\tau+C_2\,, \tag{63}$$

where the initial moment of time is $\tau_0=0$, the constants of integration are $C_1=\dot{z}_0$ and $C_2=z_0$. As a result, if the test-body is at rest at the initial moment of time ($\dot{z}_0=0$), its vertical coordinate z at another moment of observable time is

$$z=z_0-\frac{g\tau^2}{2}+\frac{v_t\tau^2}{2}\,. \tag{64}$$

The result we have obtained isn't trivial because the additional forces obtained within the framework of our theory originate in the field of the background space non-holonomity perturbed by the disc. As seen from the final equation of motion along the z-axis (62), such an additional force acts everywhere against the force of gravity. So it works like "negative gravity", a truly *anti-gravity force*.

Within the framework of Classical Mechanics we have no space-time, hence there are no space-time terms in the metrics which determine the non-holonomity of space. So such an anti-gravity force is absent in Classical Mechanics.

Such an anti-gravity force vanishes in particular cases of General Relativity, where the pseudo-Riemannian space is holonomic, and also in Special Relativity, where the pseudo-Riemannian space is holonomic by definition (in addition to the absence of curvature, gravitation, and deformation).

So the obtained anti-gravity force appears only in General Relativity, where the space is non-holonomic.

It should be noted that the anti-gravity force $F=mv_t$ isn't related to a family of forces of inertia. Inertial forces are fictitious forces unrelated to a physical field; an inertial force appears only in mechanical contact with that physical body which produces it, and disappears when the mechanical connexion ceases. On the contrary, the obtained anti-gravity force originates from a real physical field — a field of the space non-holonomity, — and is produced by the field in order to compensating for the perturbation therein. So the anti-gravity force obtained within the framework of our theory is a real physical force, in contrast to forces of inertia.

Concerning Podkletnov's experiment, we should take into account the fact that a balance suspended test-body isn't free, due to the force of reaction of the pier of the balance which completely compensates for the common force of attraction of the test-body towards the Earth (the body's weight). As a result such a test-body moves along a non-geodesic world-trajectory, so the equations of motion of such a particle have non-zero right side containing the force of the reaction of the pier. In the state of static weight, the common acceleration of the test-body in the z-direction is zero ($\ddot{z}=0$), hence its weight Q is

$$Q=mg-mv_t\,. \tag{65}$$

The quantity v_t contained in the additional anti-gravity force $F=mv_t$ is determined by the parameters of the small twists of the disc in the horizontal plane, the frequency of which is the same as the frequency Ω of vertical oscillation of the disc, while the amplitude depends on parameters of the disc, such as its radius r and the amplitude z_0 of the oscillation. (A calculation for such an anti-gravity force in the condition of a real experiment is given in the next Section. As we will see, our theory gives good coincidence with the weight-loss effect as measured in Podkletnov's experiment.)

The geodesic equation we have obtained in the field of an oscillating disc allows us to draw a final conclusion about the origin of the forces which drive the weight-loss effect in Podkletnov's experiment:

> A force produced by the field of the background space non-holonomity, compensating for a perturbation therein, works like *negative gravity* in the condition of an Earth-bound experiment. Being produced by a real physical field that bears its own energy and momentum, such an anti-gravity force is a real physical force, in contrast to fictitious forces of inertia which are unrelated to physical fields.
>
> In the conditions of Podkletnov's experiment, a horizontally placed superconducting disc, suspended in air due to an alternating magnetic field, undergoes oscillatory bounces in a vertical direction (orthogonal to the plane of the disc) with the same frequency of the magnetic field. Such an oscillation perturbs the field of the background space non-holonomity, initially homogeneous. As a result the background non-holonomity field is perturbed in three spatial directions, including the horizontal plane (the plane of the disc), resulting in small amplitude oscillatory twists about the vertical direction. The oscillatory twists determine the *anti-gravity force*, produced by the perturbed field of the background space non-holonomity, and act in the vertical directing against the force of gravity. Any test-body, placed in the perturbed non-holonomity field above such a vertically oscillating disc, should experience a loss in its weight, the numerical value of which is determined by the parameters of the disc and its oscillatory motion in the vertical direction. If such a disc rotates with acceleration, this should be the source of an addition perturbation of the background non-holonomity field and, hence, a substantial addition to the weight-loss effect should be observed in experiment. (Uniform rotation of the disc should give no effect.)

Herein we have been concerned with only a theory of a phenomenon discovered by Podkletnov (we refer to this as the *Podkletnov effect*, to fix the term in scientific terminology).

According to our theory, superconductor technology accounts in Podkletnov's experiment only for levitation of the disc and driving it into small amplitude oscillatory motion in the vertical direction. However, it is evident that this isn't the only way to achieve such a state for the disc.

Furthermore, we show that there are also both mechanical and nuclear systems which can simulate the Podkletnov effect and, hence, be the sources of continuous and explosive energy from the field of the background space non-holonomity.

Such a mechanical system, simulating the conditions of the Podkletnov effect, provides a possibile means of continuous production of energy from the space non-holonomity field. At the same time we cannot achieve high numerical values of the oscillatory motion in a mechanical system, so the continuous production of energy might be low (althopugh it may still reach useful values).

On the contrary, processes of nuclear decay and synthesis, due to the instant change of the spin configuration among nucleons inside nuclei, should have high numerical values of v_t, and therefore be an explosive source of energy from the field of the background space non-holonomity.

Both mechanical and nuclear simulations of the Podkletnov effect can be achieved in practice.

4 A new experiment proposed on the basis of the theory

4.1 A simple test of the theory of the Podkletnov effect (alternative to superconductor technology)

According our theory, the Podkletnov effect has a purely mechanical origin, unrelated to superconductivity — the field of the background space non-holonomity being perturbed by a disc which undergoes oscillatory bounces orthogonal to its own plane, produces energy and momentum flow in order to compensate for the perturbation therein. Owing to this, we propose a purely mechanical experiment which reproduces the Podkletnov effect, equivalent to Podkletnov's original superconductor experiment, which would be a cheap alternative to costly superconductor technology, and also be a simple mechanical test of the whole theory of the effect.

What is the arrangement of such a purely mechanical system, which could enable reproduction of the Podkletnov effect? Searching the scientific literature, we found such a system. This is the *vibration balance* [22], invented and tested in the 1960–1970's by N. A. Kozyrev, a famous astronomer and experimental physicist of the Pulkovo Astronomical Observatory (St. Petersburg, Russia). Below is a description of the balance, extracted from Kozyrev's paper [22]:

> "The vibration balance is an equal-shoulder balance, where the pier of the central prism is connected to a vibration machine. This vibration machine produces vertical vibration of the pier. The acceleration of the vibration is smaller than the acceleration of the Earth's gravitation. Therefore the prism doesn't lose contact with the pier, only alternating pressure results. Thus the distance between the centre of gravity and the cone of the prism remains constant while the weight and the balance don't change their own measurement precision. The vertical guiding rods, set up along the pier, exclude the possibility of horizontal motion of the pier. One of two samples of the same mass is rigidly suspended by the yoke of the balance, while the second sample is suspended by an elastic material. Here the force required to lift the yoke is just a small percentage of the force required to lift the rigidly fixed sample. Therefore, during vibration of the balance, there is stable kinematic of the yoke, where the point O (the point of hard suspension)

doesn't participate in vibration, while the point A (the point of elastic suspension) has maximal amplitude of oscillation which is double the amplitude of the central prism C. Because the additional force, produced during vibration, is just a few percent more than the static force, the yoke remains fixed without inner oscillation, i.e. without twist, in accordance with the requirement of static weight.

We tested different arrangements of balances under vibration. The tested balances had different sensitivities, while the elastic material was tried with rubber, a spring, etc. Here is detailed a description of the vibration balance which is currently in use. This is a technical balance of the second class of sensitivity, with a maximum payload of 1 kg. A 1 mm deviation of the measurement arrow, fixed on the yoke, shows a weight of 10 mg. The centre of gravity of the yoke is located ∼1 cm below the pier of the central prism. The length of the shoulders of the yoke is: $OC = CA = l = 16$ cm. The amplitude of vibration is $a \approx 0.2$ mm. Thus the maximum speed of the central prism is $v = \frac{2\pi}{T}a \simeq 2$ cm/sec, while its maximum acceleration $\left(\frac{2\pi}{T}\right)^2 a = 2\times10^2$ is about 20% of the acceleration of the Earth's gravitation. We regularly used samples of 700 g. One of the samples was suspended by a rubber, the strain of which for 1 cm corresponds 100 g weight. So, during vibration, the additional force on the yoke is less than 10 g and cannot destroy the rigidity of the yoke. The elastic rubber suspension absorbs vibration so that the sample actually rests.

This balance, as well as all recently tested systems, showed each time the increase of the weight of the elastically suspended sample. This additional force $\triangle Q$ is proportional to the weight of the sample Q, besides $\triangle Q/Q = 3\times10^{-5}$. Hence, having $Q = 700$ g, $\triangle Q = 21$ mg and the force momentum twisting the yoke is 300 dynes×cm.

[...] From first view one can think that, during such a vibration, the pier makes twists around the resting point O. In a real situation the points of the pier are carried into more complicated motion. The central prism doesn't lose contact with the pier; they are connected, and move only linearly. Therefore the central part of the yoke, where its main mass is concentrated, has no centrifugal acceleration. What is about the point O, this point in common with the rigidly suspended sample is fixed in only the vertical direction, but it can move freely in the horizontal direction. These horizontal displacements of the point O are very small. Naturally, they are $\frac{a^2}{2l}$, i.e. $\sim 0.1\,\mu$m in our case. Despite that, the small displacements result a very specific kinematic of the yoke. During vibration, each point of the yoke draws an element of an ellipse, a small axis of which lies along the yoke (in the average position of it). The concavities of the elements in the yoke's sections O–C and C–A are directed opposite to each other; they produce oppositely directed centrifugal forces. Because $\bar{v}^2$ is greater in the section C–A, the centrifugal forces don't compensate each other completely: as a result there in the yoke a centrifugal force acts in the A-direction (the direction at the point of the elastically suspended sample). This centrifugal acceleration has maximum value at the point A. We have $\bar{v}^2 = \frac{4\pi^2}{T^2}a^2 = 6$ cm²/sec². From here we obtain the curvature radius of the ellipse: $\rho = 4l = 60$ cm. So the centrifugal acceleration is $\frac{\bar{v}^2}{\rho} = 0.1$ cm/sec²."

Such a vibration balance is shown in the upper picture of Fig. 4. An analogous vibration balance is shown in the lower picture of Fig. 4: there the vibration machine is connected not to the pier of the central prism, but to he elastic suspension, while the prism's pier is supported by a spring; such a system should produce the same effect.

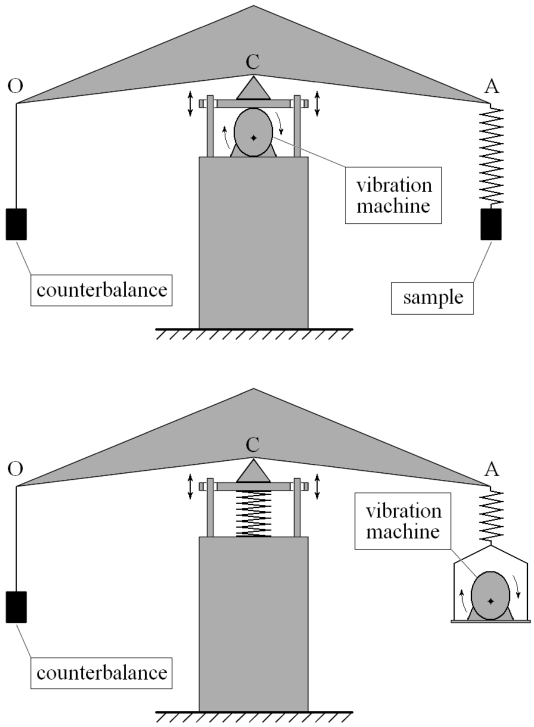

Fig. 4: The vibration balance — a mechanical test of the whole theory of the Podkletnov effect (a simple alternative to costly superconductor technology).

To understand how the Podkletnov effect manifests with the vibration balance, we consider the operation of the balance in detail (see Fig. 5).

The point O of the yoke undergoes oscillatory bounces in the r-direction with the amplitude d, given by

$$d = l - l\cos\alpha = l - l\sqrt{1-\sin^2\!\alpha} = \\ = l - l\sqrt{1-\frac{a^2}{l^2}} \simeq l - l\left(1-\frac{a^2}{2l^2}\right) \simeq \frac{a^2}{2l}\,, \tag{66}$$

while b is

$$b = d\tan\alpha = d\,\frac{a}{l\cos\alpha} \simeq \frac{a^3}{2l^2\left(1-\frac{a^2}{2l^2}\right)} \simeq \frac{a^3}{2l^2-a^2}\,. \tag{67}$$

The point A undergoes oscillatory bounces in the z-direction with the amplitude $2a$, while its oscillatory motion in the r-direction has the amplitude

$$c = 2l - 2l\cos\alpha - d = d\,. \tag{68}$$

The oscillatory bouncing of the points O and A along the elements of an ellipse is an accelerating/decelerating rotational motion around the focus of the ellipse. In such a case, by definition of the space non-holonomity as the non-orthogonality of time lines to the spatial section, manifest

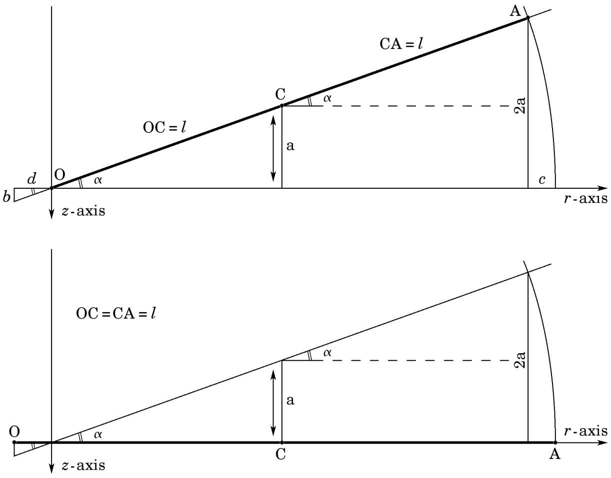

Fig. 5: The yoke of the vibration balance in operation. The yoke OA is indicated by the bold line. The double arrow shows the oscillatory bouncing motion of the point C, which is the point of connexion of the central prism and the central point of the yoke. The lower picture shows the yoke in its initial horizontal position. The upper picture shows the yoke in the upper position, at maximum deviation from the state of equilibrium.

as a three-dimensional rotation, points O and A during the oscillatory motion along respective elliptic elements, are the *source of a local field of the space non-holonomity*. Respective tangential accelerations $\bar{v}_t$ at the points O and A determine the sources.

Given that the background space is non-holonomic, such a field of the local non-holonomity is a *perturbation field* in the non-holonomic background. In other words, points O and A, in common with the respective samples mechanically connected to the points, are the sources of respective perturbation fields in the background field of the space non-holonomity.

Each point of the yoke, being carried into such an oscillatory motion, is the source of such a perturbation field. On the other hand, the average tangential acceleration of the motion, $\bar{v}_t$, takes its maximum value at the point A, then substantially decreases to the point O where it is negligible. Therefore such a yoke can be approximated as a non-symmetric system, where the end-point A is the source of a perturbation field in the non-holonomic background, while the end-point O isn't such a source.

According to the Einstein equations we have obtained in (35), the energy and momentum of a perturbation field in the non-holonomic background are produced by the whole field of the background space non-holonomity in order to compensate for the perturbation therein*. So the energy produced on a test-body in such a perturbation field isn't limited by the energy of the source of the perturbation (an oscillator, for instance), but can increase infinitely.

According to the geodesic equations (61) we have obtained in a perturbed non-holonomic field, the momentum of such a perturbation field manifests as the additional forces which act in all three directions r, φ, z relative to the source of the perturbation. If considering a free test-body constrained to move only along only the Earth's gravitational field-lines (falling freely in the z-direction), such an add-on force is expressed in the geodesic equation along the z-axis (62)

$$\ddot{z} + g - v_t = 0 \tag{69}$$

as $F = m v_t$, and works against the force of gravity mg. In the situation of a static weight the total acceleration of such a sample is zero, $\ddot{z} = 0$, while the other forces are put into equilibrium by the weight of the sample (65)

$$Q = mg - m v_t = Q_0 - \triangle Q\,. \tag{70}$$

A source of perturbation cannot be an object of application of a force produced due to the perturbation. Therefore the sample O is the object of application of an anti-gravity force $F = m v_t$ due to a field of the anti-gravity accelerations v_t, a source of which is the oscillatory bouncing system of the point A in common with the elastically suspended sample, while the point A itself in common with the sample has no such anti-gravity force applied to it. As a result the weight of the sample rigidly suspended at the end-point O, decreases as $\triangle Q = m v_t$, while the weight of the sample A remains the same:

$$Q_{\rm O} = mg - m v_t\,, \qquad Q_{\rm A} = mg\,. \tag{71}$$

As a result, such a balance, during its vibration, should demonstrate a weight-loss of the rigidly suspended sample O and, respectively, a twist of the balance's yoke to the elastically suspended sample A. Such a weight-loss effect on the rigidly suspended sample, which is a fictitious increase of the weight of the elastically suspended sample, was first observed during the years 1960–1970's in the pioneering experiment of Kozyrev [22].

The half-length horizontal section of a superconducting disc suspended in air by an alternating magnetic field in Podkletnov's experiment (see Fig. 2) can be approximated by the yoke of the aforementioned vibrational balance. This is because the vertical oscillation of such a disc by an alternating magnetic field isn't symmetric in the disc's plane, so such a disc has a small oscillatory twisting motion in the vertical plane to the yoke of the vibration balance†.

*Note that we deduced the Einstein equations (35) for a space pervaded not only by an electromagnetic field, but also by distributed matter characterised by arbitrary properties. If only an electromagnetic field, there would be $\rho c^2 = U$. However $\rho c^2 - U \neq 0$ in the Einstein equations (35). This can be due to a number of reasons, the presence of an elastic force which compresses a spring, for instance. Therefore the Einstein equations we have obtained (35) are applicable to a laboratory space containing such a vibration balance.

†This is despite the fact that such a disc has so small an amplitude and so high a frequency of oscillatory twisting motion, that it seems to be levitating when almost at rest.

As a result, such a disc should experience the anti-gravity force $F = mv_t$ at the end-points of the disc, along the whole perimeter. Common action of the forces should produce:

1. The weight-loss effect $\triangle Q = mv_t$ on the disc itself. The weight-loss of the disc should increase if the disc has accelerating/decelerating rotation;
2. Respective weight-loss effect on any test-body located over the disc along the vertical axis z, according to the field of anti-gravity accelerations v_t.

Therefore the disc in Podkletnov's experiment and a vibration balance of the aforementioned type are equivalent systems. So both the superconductor experiment and the vibration balance should be described by the same theory we have adduced herein, and produce the same weight-loss effect as predicted by the theory.

The numerical value of such an anti-gravity acceleration, v_t, can also be calculated within the framework of our theory of the Podkletnov effect, and thus checked in experiment.

According to our theory, the value v of the perturbation isn't dependent on the vertical direction (the z-direction in our coordinates). Therefore only the horizontal oscillatory bouncing motion of point A (in common with the sample rigidly suspended there) perturbs the background field of the space non-holonomity. According to Fig. 5, the tangential acceleration of the point A in its oscillatory motion with amplitude $2a$ along an ellipse with the radius $\rho = 4l$, is directed in the z-direction. So the tangential acceleration cannot perturb the non-holonomic background. However there is another tangential acceleration of the point A, which results from the oscillatory motion of the point with the amplitude c (numerically $c = d$) around the upper location of the point A. This tangential acceleration is directed along the r-axis, so it is the source of a local perturbation in the non-holonomic background. The angle of the small twist at the point A during such an oscillation is $\varphi = \frac{d}{2\pi a} = \frac{a}{4\pi l}$, so the average angular acceleration of the motion is $\bar{\ddot{\varphi}} = \frac{1}{2}\ddot{\varphi} = \frac{\Omega^2 a}{8\pi l}$. The average tangential acceleration of the motion, directed in the r-direction, is $\bar{v}_t = 2a\bar{\ddot{\varphi}}$, i.e.

$$\bar{v}_t = \frac{\Omega^2 a^2}{4\pi l} = \frac{\pi \nu^2 a^2}{l}\,, \tag{72}$$

which characterizes, according to the definition of the space non-holonomity, the local perturbation in the background field of the space non-holonomity.

Consider a vibration balance like that in Kozyrev's original experiment [22]. Each shoulder of the yoke has the length $l = 16$ cm, so the total length of the yoke is 32 cm. Let the central prism of the balance undergo oscillatory bounces in the vertical direction with an amplitude of $a = 0.020$ cm, so the amplitude of the point A is $2a = 0.040$ cm. One of the samples is rigidly suspended at point O of the yoke, while the other sample is suspended at point A by an elastic medium. Both samples have the same mass: 700 g. According to our theory, the Podkletnov effect should appear in the balance as a weight loss $\triangle Q$ of the sample O, dependent on the frequency as follows:

ν, Hz	v_t, cm/sec^2	$\triangle Q/Q$	$\triangle Q$, mg	$\triangle Q_{\text{exp}}$, mg
30	0.071	7.2×10^{-5}	50	
25	0.049	5.0×10^{-5}	35	
20	0.031	3.2×10^{-5}	22	21
15	0.018	1.8×10^{-5}	13	
10	0.0079	8.0×10^{-6}	5.6	

Table 1: The weight-loss effect, calculated with our theory of the Podkletnov effect, for a vibration balance with the same characteristics as that of Kozyrev's pioneering experiment [22]. The last column gives the numerical value of the weight-loss effect observed in Kozyrev's experiment, at a constant frequency of 20 Hz.

Kozyrev measured $\triangle Q = 21$ mg at a fixed frequency of $\nu = 20$ Hz in his experiment [22]. This corresponds with $\triangle Q = 22$ mg predicted by our theory*.

For Podkletnov's experiment, we haven't enough data for the amplitude of oscillatory bouncing motion of the superconductor disc. Despite this, we can verify our theory of the phenomenon in another way, due to the fact that Podkletnov observed a dependence of the weight-loss effect on the oscillation frequency.

Although dependency on frequency was observed in each of Podkletnov's experiments, we only have detailed data for the 1997 experiment, from publication [2]. We give in Table 2 Podkletnov's experimental values of $\triangle Q/Q$, measured on a sample located in the field of a 275/80 × 10 mm superconductor toroid at vibration frequencies of the toroid from 3.1 MHz to 3.6 MHz and the constant rotation speed 4300 rpm. The last column gives the increasing values of $\triangle Q/Q$, calculated by our theory where the weight-loss effect should be dependent on the square of the vibration frequency:

ν, MHz	$(\triangle Q/Q)_{\text{exp}}$	$(\triangle Q/Q)_{\text{theor}}$
3.1	2.2×10^{-3}	
3.2	2.3×10^{-3}	2.3×10^{-3}
3.3	2.4×10^{-3}	2.5×10^{-3}
3.4	2.6×10^{-3}	2.6×10^{-3}
3.5	2.9×10^{-3}	2.8×10^{-3}
3.6	3.2×10^{-3}	3.0×10^{-3}

Table 2: The increase of the weight-loss effect $(\triangle Q/Q)_{\text{exp}}$ with vibration frequency ν, measured in Podkletnov's experiment of 1997 [2], in comparison to the value $(\triangle Q/Q)_{\text{theor}}$ calculated by our theory of the phenomenon.

*We should also add that, coming from the geodesic equation along the z-axis, which is the third equation of (61), to the simplified form (62) thereof, we omitted the harmonic term from consideration. If the term is included, the vibration balance experiment should reveal not only an increase of the weight-loss effect with the frequency, but also resonant levels in it. The resonant levels, in further experiment, would be an additional verification of our theory.

We see that our theory is in very close accord with Podkletnov's experimental data. Furthermore, according to Podkletnov [2], despite the high measurement precision of the balance used in his experiment, some error sources produced systematic error in the order of 10^{-3} during the experiment. Taking this into account, we conclude that our theory is *sufficiently coincident* with Podkletnov's experimental data.

Podkletnov observed a decrease of the air pressure over the working device in the laboratory, and also a force distributed in a radial direction. We point out that the geodesic equations (61) obtained within the framework of our theory show forces, aside for the vertically acting anti-gravity force (i.e. acting in the z-direction), acting in the directions r and φ as well, produced by the perturbed field of the space non-holonomity. We therefore interpret Podkletnov's observations as a qualitative verification of our theory.

Podkletnov measured a much greater weight-loss effect over a disc during its accelerating/braking rotation. We haven't developed a theory for a rotating disc yet. Despite that, by analogy with our theory for a non-rotating disc, we can qualitatively predict that a field of the anti-gravity acceleration v_t produced by a rotating disc should be proportional to the radius of the disc and its angular acceleration, in accordance with the fact that Podkletnov's experiment is very difficult to reproduce on small discs, diameter about $1''$. Following Podkletnov, the weight-loss effect will be surely measured on a disc of at least $5''$ diameter.

Finally, complete verification of our theory of the Podkletnov effect should usher in new experimental checks for the frequency dependency of the weight-loss, which should appear in both the vibration balance and the Podkletnov superconductor device. With a new vibration balance experiment and a superconductor experiment confirming the frequency dependency according to (72), our theory of the Podkletnov effect would be completely verified.

4.2 New energy sources and applications to space travel

Due to the predictions of our theory, we have the possibility of the Podkletnov effect on such a simple device as the vibration balance, which is a thousand times cheaper and accessible than superconductor technology. In other words, being armed with the theory, it is more reasonable to use the weight-loss effect in practice with other devices which, working on principles other than the Podkletnov superconductor device, could easily reproduce the effect in both an Earth-bound laboratory and in space.

On the basis of our theory, new engineering applications such as anti-gravity devices and devices which could be used as new sources of energy, might be developed.

Anti-gravity engines for air and space travel. There can be at least two kinds of such engines, projected on the basis of our theory:

1. Land-based engines, which produce a strong anti-gravity acceleration field due to the Podkletnov effect. The anti-gravity acceleration field doesn't depend on the vertical distance from the disc, which generates it in Podkletnov's experiment. Due to this fact, a land-based engine, producing a beam of the anti-gravity acceleration field focused on a flying apparatus, can be used by the flying vehicle as a power station. The anti-gravity acceleration in the beam becomes the same as the acceleration of free fall. There can be limitation only from the scattering of the beam with distance. So such a land-based engine is suitable for short distances used in air travel*;
2. Engines located on board of a flying vehicle, that can be more suitable for both air and space travel. Such an engine, being the source of a field of the anti-gravity acceleration, cannot be the subject of application of the anti-gravity force produced in the field. However the force applies to the other parts of the apparatus, as in the vibration balance experiment or Podkletnov's experiment.

We note that in both cases, it isn't necessary to use a purely mechanical kernel for such an engine, as for the vibration balance experiment and Podkletnov's experiment considered in this paper. Naturally, using a mechanical oscillatory bouncing motion or accelerating/braking rotation, the maximum acceleration in the generated anti-gravity field is limited by the shock resistance of the mechanical aspects of the engine. This substantial limitation can be overcome if instead of solid bodies, liquids (liquid metal like mercury, for instance) or liquid crystals are driven into such motion by high frequency electromagnetic fields.

Devices which could be the source of new energy. This is another application of our theory, the experimental realization of which differs from the vibration balance experiment and Podkletnov's experiment. According to our theory, the coupling energy between the nucleons in a nucleus should be different due to the Podkletnov effect depending on the common orientation of the nucleons' spins in the nucleus. As a result, we could have a large explosive production of energy during not only self-decay of heavy elements like uranium and the trans-uraniums, but also by destroying the nuclei of the lightweight elements located in the middle of the Periodic Table of Elements. Of course, not just any nucleus will be the source of such energy production, but only those where, by our theory, the Podkletnov effect works, due to the specific orientation of the spins in the strong interaction amongst the nucleons.

Such an energy source, being free of deadly radiation or radioactive waste, could be a viable alternative to nuclear power plants.

*This kind of anti-gravity engine was first proposed in 2006 by Eugene Podklenov, in his interview [8].

Acknowledgements

We dedicate this research to the memory of Prof. Kyril Stanyukovich (1916–1989) and Dr. Abraham Zelmanov (1913–1987), ours teachers, and also Prof. Nikolai Kozyrev (1908–1983) and Dr. Roberto di Bartini (1897–1974) whose influence on our scientific views has been so great.

We also are very thankful to Delyan Zhelyazov for a few typing mistakes found by him in the formulae when this issue was sent to print.

Submitted on May 21, 2007
Accepted on May 31, 2007
Corrected online on December 08, 2007

References

1. Podkletnov E. and Nieminen R. A possibility of gravitational force shielding by bulk $YBa_2Cu_3O_{7\text{-}x}$ superconductor. *Physica C*, v. 203, 1992, 441–444.
2. Podkletnov E. Weak gravitation shielding properties of composite bulk $YBa_2Cu_3O_{7\text{-}x}$ superconductor below 70 K under e. m. field. arXiv: cond-mat/9701074.
3. Seife C. NASA is spending over half a million dollars on bizarre antigravity research. *New Scientist Magazine*, Issue 2172, February 06, 1999.
4. Wertheim M. Defying the shackles of gravity is a dream enshrined in myth and the human psyche. Now NASA will test a machine to determine if it is also real science. *Los Angeles Times*, March 24, 2002.
5. Boeing tries to defy gravity: an anti-gravity device would revolutionise air travel. *BBC News*, Monday, July 29, 2002.
6. Cohen D. Anti-gravity research on the rise. *New Scientist News*, July 30, 2002.
7. Ball Ph. Antigravity craft slips past patent officers: “Impossible” device gets seal of approval. *Nature*, v. 438, November 10, 2005, 139.
8. Ventura T. Interview with Dr. Eugene Podkletnov, April 10, 2006. It is accessed on http://www.americanantigravity.com/documents/Podkletnov-Interview.pdf
9. Podkletnov E. and Modanese G. Impulse gravity generator based on charged $YBa_2Cu_3O_{7\text{-}y}$ superconductor with composite crystal structure. arXiv: physics/0108005.
10. Alexandrov P. S. Combinatorial topology. Dover Publications, Mineola (NY), 1998 (rep. from the first edition of 1947).
11. Oros di Bartini R. Some relations between physical constants. *Doklady Acad. Nauk USSR*, 1965, v. 163, No. 4, 861–864.
12. Oros di Bartini R. Relations between physical constants. *Problems of the Theory of Gravitation and Elementary Particles*, Ed. by K. P. Stanyukovich and H. A. Sokolik, Moscow, Atomizdat, 1966, 249–266.
13. Oros di Bartini R. Relations between physical constants. *Progress in Physics*, 2005, v. 3, 34–40.
14. Raschewski P. K. Riemannsche Geometrie und Tensoranalysis. Deutsche Verlag der Wissenschaften, Berlin, 1959.
15. Zelmanov A. L. Chronometric invariants. Dissertation thesis, 1944. American Research Press, Rehoboth (NM), 2006.
16. Zelmanov A. L. Chronometric invariants and co-moving coordinates in the general relativity theory. *Doklady Acad. Nauk USSR*, 1956, v. 107(6), 815–818.
17. Rabounski D. Zelmanov’s anthropic principle and the infinite relativity principle. *Progress in Physics*, 2005, v. 1, 35–37.
18. Gabrielse G., Hanneke D., Kinoshita T., Nio M. and Odom B. New determination of the fine structure constant from the electron g value and QED. *Phys. Rev. Lett.*, 2006, v. 97, 030802.
19. Petrov A. Z. Einstein spaces. Pergamon Press, Oxford, 1969, 411 pages (transl. by R. F. Kelleher, ed. by J. Woodrow).
20. Landau L. D. and Lifshitz E. M. The classical theory of fields. Butterworth–Heinemann, 2003, 428 pages (4th edition).
21. Lefschetz S. Differential equations: geometric theory. Interscience Publishers, New York, 1957.
22. Kozyrev N. A. The vibration balance and analysis of its operation. *Problems of Research of the Universe*, v. 7: “Astrometry and Celestial Mechanics”, Moscow-Leningrad, 1978, 582–584.
23. Peres A. On geometrodynamics and null fields. *Annals of Physics* (N.Y.), 1961, v. 14(1), 419–439.
24. Wheeler J. A. Geometrodynamics. Academic Press, N.Y., 1962.
25. Caltenco Franca J. H., López-Bonilla J. L. and Peña-Rivero R. The algebraic Rainich conditions. *Progress in Physics*, 2007, v. 3, 50–51.
26. Nordtvedt K. and Pagels H. Electromagnetic plane wave solutions in general relativity. *Annals of Physics* (N.Y.), 1962, v. 17(3), 426–435.
27. Rabounski D. A theory of gravity like electrodynamics. *Progress in Physics*, 2005, v. 2, 15–29.

Appendix 1 The space non-holonomity as rotation

How is the non-orthogonality of the coordinate axes expressed by the components of the fundamental metric tensor $g_{\alpha\beta}$? To show this there are a few ways [14]. We use a formal method developed by Zelmanov [15]. First, we introduce a *locally geodesic reference frame* at a given point of the Riemannian space. Within infinitesimal vicinities of any point of such a reference frame the fundamental metric tensor is

$$\tilde{g}_{\alpha\beta} = g_{\alpha\beta} + \frac{1}{2}\left(\frac{\partial^2 \tilde{g}_{\alpha\beta}}{\partial\tilde{x}^\mu \partial\tilde{x}^\nu}\right)(\tilde{x}^\mu - x^\mu)(\tilde{x}^\nu - x^\nu) + \ldots,$$

i. e. the components at a point, and in its vicinity, are different from those at the point of reflection to within only the higher order terms, the values of which can be neglected. Therefore, at any point of a locally geodesic reference frame the fundamental metric tensor can be considered constant, while the first derivatives of the metric (the Christoffel symbols) are zero.

As a matter of fact, within infinitesimal vicinities of any point located in a Riemannian space, a locally geodesic reference frame can be set up. At the same time, at any point of this locally geodesic reference frame a tangentially flat Euclidean space can be set up so that this reference frame, being locally geodesic for the Riemannian space, is the global geodesic for that tangential flat space.

The fundamental metric tensor of a flat Euclidean space is constant, so the values of $\tilde{g}_{\mu\nu}$, taken in the vicinity of a point of the Riemannian space, converge to the values of the tensor $g_{\mu\nu}$ in the flat space tangential at this point. Actually, this means that we can build a system of basis vectors $\vec{e}_{(\alpha)}$, located in this flat space, tangential to curved coordinate lines of the Riemannian space.

In general, coordinate lines in Riemannian spaces are curved, inhomogeneous, and are not orthogonal to each other. So the lengths of the basis vectors may sometimes be very different from unity.

We denote a four-dimensional infinitesimal displacement vector by $d\vec{r} = (dx^0, dx^1, dx^2, dx^3)$, so that $d\vec{r} = \vec{e}_{(\alpha)} dx^\alpha$, where components of the basis vectors $\vec{e}_{(\alpha)}$ tangential to the coordinate lines are $\vec{e}_{(0)} = \{e^0_{(0)}, 0, 0, 0\}$, $\vec{e}_{(1)} = \{0, e^1_{(1)}, 0, 0\}$, $\vec{e}_{(2)} = \{0, 0, e^2_{(2)}, 0\}$, $\vec{e}_{(3)} = \{0, 0, 0, e^2_{(3)}\}$. The scalar product of the vector $d\vec{r}$ with itself is $d\vec{r}d\vec{r} = ds^2$. On the other hand, the same quantity is $ds^2 = g_{\alpha\beta}\, dx^\alpha dx^\beta$. As a result we have

$$g_{\alpha\beta} = \vec{e}_{(\alpha)}\vec{e}_{(\beta)} = e_{(\alpha)} e_{(\beta)} \cos\left(x^\alpha; x^\beta\right),$$

so we obtain

$$g_{00} = e^2_{(0)}\,,$$
$$g_{0i} = e_{(0)} e_{(i)} \cos\left(x^0; x^i\right),$$
$$g_{ik} = e_{(i)} e_{(k)} \cos\left(x^i; x^k\right).$$

The gravitational potential is $\mathrm{w} = c^2(1 - \sqrt{g_{00}})$. So the time basis vector $\vec{e}_{(0)}$ tangential to the time line $x^0 = ct$, having the length

$$e_{(0)} = \sqrt{g_{00}} = 1 - \frac{\mathrm{w}}{c^2}\,,$$

is smaller than unity the greater the gravitational potential w.

The space rotation linear velocity $v_i = -\frac{c\, g_{0i}}{\sqrt{g_{00}}}$ and, according to it, the chr.inv.-metric tensor $h_{ik} = -\, g_{ik} + \frac{g_{0i}\, g_{0k}}{g_{00}}$ gives

$$v_i = -\, c\, e_{(i)} \cos\left(x^0; x^i\right),$$
$$h_{ik} = e_{(i)} e_{(k)} \Big[\cos\left(x^0; x^i\right) \cos\left(x^0; x^k\right) - \cos\left(x^i; x^k\right)\Big].$$

Appendix 2 A short tour of chronometric invariants

Determination of physical observable quantities in General Relativity isn't a trivial problem. For instance, for a four-dimensional vector Q^α we may heuristically assume that its three spatial components form a three-dimensional observable vector, while the temporal component is an observable potential of the vector field (which generally doesn't prove they can be actually observed). However a contravariant tensor of the 2nd rank $Q^{\alpha\beta}$ (as many as 16 components) makes the problem much more indefinite. For tensors of higher rank the problem of heuristic determination of observable components is more complicated. Besides, there is an obstacle related to definition of observable components of covariant tensors (in which the indices are subscripts) and of mixed tensors, which have both subscripts and superscripts. Therefore the most reasonable way out of the labyrinth of heuristic guesses is to create a strict mathematical theory to enable calculation of observable components for any tensor quantities.

A complete mathematical apparatus to calculate physical observable quantities for a four-dimensional pseudo-Riemannian space was completed in 1944 by Abraham Zelmanov [15]: that is the strict solution of the problem. He called the apparatus the *theory of chronometric invariants*. Many researchers were working on the problem in the 1930–1940's. Even Landau and Lifshitz in their famous book *The Classical Theory of Fields* (1939) introduced observable time and the observable three-dimensional interval similar to those introduced by Zelmanov. But they limited themselves only to this particular case and did not arrive at general mathematical methods to define physical observable quantities in pseudo-Riemannian spaces.

The essence of Zelmanov's theory is that if an observer accompanies his physical reference body, his observable quantities are projections of four-dimensional quantities on his time line and the spatial section — *chronometrically invariant quantities*, made by projecting operators

$$b^\alpha = \frac{dx^\alpha}{ds}\,, \qquad h_{\alpha\beta} = -\, g_{\alpha\beta} + b_\alpha b_\beta\,,$$

which fully define his real reference space (here b^α is his velocity with respect to his real references). Thus, the chr.inv.-projections of a world-vector Q^α are

$$b_\alpha Q^\alpha = \frac{Q_0}{\sqrt{g_{00}}}\,, \qquad h^i_\alpha Q^\alpha = Q^i,$$

while chr.inv.-projections of a world-tensor of the 2nd rank $Q^{\alpha\beta}$ are

$$b^\alpha b^\beta Q_{\alpha\beta} = \frac{Q_{00}}{g_{00}}\,, \quad h^{i\alpha} b^\beta Q_{\alpha\beta} = \frac{Q^i_0}{\sqrt{g_{00}}}\,, \quad h^i_\alpha h^k_\beta Q^{\alpha\beta} = Q^{ik}.$$

Physically observable properties of the space are derived from the fact that chr.inv.-differential operators

$$\frac{{}^*\partial}{\partial t} = \frac{1}{\sqrt{g_{00}}}\frac{\partial}{\partial t}\,, \qquad \frac{{}^*\partial}{\partial x^i} = \frac{\partial}{\partial x^i} + \frac{1}{c^2}\, v_i \frac{{}^*\partial}{\partial t}$$

are non-commutative

$$\frac{{}^*\partial^2}{\partial x^i\, \partial t} - \frac{{}^*\partial^2}{\partial t\, \partial x^i} = \frac{1}{c^2} F_i \frac{{}^*\partial}{\partial t}\,, \quad \frac{{}^*\partial^2}{\partial x^i \partial x^k} - \frac{{}^*\partial^2}{\partial x^k \partial x^i} = \frac{2}{c^2} A_{ik} \frac{{}^*\partial}{\partial t}\,,$$

and also from the fact that the chr.inv.-metric tensor

$$h_{ik} = -\, g_{ik} + \frac{g_{0i}\, g_{0k}}{g_{00}} = -\, g_{ik} + \frac{1}{c^2}\, v_i v_k\,,$$

which is the chr.inv.-projection of the fundamental metric tensor $g_{\alpha\beta}$ onto the spatial section $h^\alpha_i h^\beta_k\, g_{\alpha\beta} = -\, h_{ik}$, may not be stationary. The main observable characteristics are the chr.inv.-vector of gravitational inertial force F_i, the chr.inv.-tensor of angular velocities of the space rotation A_{ik}, and the chr.inv.-tensor of rates of the space deformations D_{ik}, namely

$$F_i = \frac{1}{\sqrt{g_{00}}}\left(\frac{\partial \mathrm{w}}{\partial x^i} - \frac{\partial v_i}{\partial t}\right),$$

$$A_{ik} = \frac{1}{2}\left(\frac{\partial v_k}{\partial x^i} - \frac{\partial v_i}{\partial x^k}\right) + \frac{1}{2c^2}\left(F_i v_k - F_k v_i\right),$$

$$D_{ik} = \frac{1}{2}\frac{{}^*\partial h_{ik}}{\partial t}\,, \quad D^{ik} = -\frac{1}{2}\frac{{}^*\partial h^{ik}}{\partial t}\,, \quad D = D^k_k = \frac{{}^*\partial \ln\sqrt{h}}{\partial t}\,,$$

where w is the gravitational potential

$$\mathrm{w} = c^2 \left(1 - \sqrt{g_{00}}\right),$$

and v_i is the linear velocity of the space rotation

$$v_i = -\, c\, \frac{g_{0i}}{\sqrt{g_{00}}}\,, \quad v^i = -\, c\, g^{0i} \sqrt{g_{00}}\,, \quad v_i = h_{ik} v^k,$$

while $h = \det\|h_{ik}\|$, $h g_{00} = -g$, $g = \det\|g_{\alpha\beta}\|$. Observable inhomogeneity of the space is set up by the chr.inv.-Christoffel symbols

$$\Delta^i_{jk} = h^{im} \Delta_{jk,m} = \frac{1}{2}\, h^{im}\left(\frac{{}^*\partial h_{jm}}{\partial x^k} + \frac{{}^*\partial h_{km}}{\partial x^j} - \frac{{}^*\partial h_{jk}}{\partial x^m}\right),$$

which are built just like Christoffel's usual symbols

$$\Gamma^\alpha_{\mu\nu} = g^{\alpha\sigma}\, \Gamma_{\mu\nu,\sigma} = \frac{1}{2}\, g^{\alpha\sigma}\left(\frac{\partial g_{\mu\sigma}}{\partial x^\nu} + \frac{\partial g_{\nu\sigma}}{\partial x^\mu} - \frac{\partial g_{\mu\nu}}{\partial x^\sigma}\right)$$

using h_{ik} instead of $g_{\alpha\beta}$. Components of the usual Christoffel symbols are linked to the chr.inv.-Christoffel symbols and other chr.inv.-chractersitics of the accompanying reference space of the given observer by the relations

$$D^i_k + A^{\cdot i}_{k\cdot} = \frac{c}{\sqrt{g_{00}}}\left(\Gamma^i_{0k} - \frac{g_{0k}\Gamma^i_{00}}{g_{00}}\right),$$

$$F^k = -\frac{c^2\,\Gamma^k_{00}}{g_{00}}\,, \qquad g^{i\alpha} g^{k\beta}\, \Gamma^m_{\alpha\beta} = h^{iq} h^{ks} \Delta^m_{qs}\,.$$

Zelmanov had also found that the chr.inv.-quantities F_i and A_{ik} are linked to one another by two identities

$$\frac{{}^*\partial A_{ik}}{\partial t} + \frac{1}{2}\left(\frac{{}^*\partial F_k}{\partial x^i} - \frac{{}^*\partial F_i}{\partial x^k}\right) = 0\,,$$

$$\frac{{}^*\partial A_{km}}{\partial x^i} + \frac{{}^*\partial A_{mi}}{\partial x^k} + \frac{{}^*\partial A_{ik}}{\partial x^m} + \frac{1}{2}\left(F_i A_{km} + F_k A_{mi} + F_m A_{ik}\right) = 0$$

which are known as *Zelmanov's identities*.

Zelmanov deduced chr.inv.-formulae for the space curvature. He followed that procedure by which the Riemann-Christoffel tensor was built: proceeding from the non-commutativity of the second derivatives of an arbitrary vector

$$^*\nabla_i {}^*\nabla_k Q_l - {}^*\nabla_k {}^*\nabla_i Q_l = \frac{2A_{ik}}{c^2}\frac{^*\partial Q_l}{\partial t} + H_{lki\cdot}^{\cdots j}\, Q_j\,,$$

he obtained the chr.inv.-tensor

$$H_{lki\cdot}^{\cdots j} = \frac{^*\partial \Delta_{il}^{j}}{\partial x^k} - \frac{^*\partial \Delta_{kl}^{j}}{\partial x^i} + \Delta_{il}^{m}\,\Delta_{km}^{j} - \Delta_{kl}^{m}\,\Delta_{im}^{j}$$

which is similar to Schouten's tensor from the theory of non-holonomic manifolds. The tensor $H_{lki}^{\cdots j}$ differs algebraically from the Riemann-Christoffel tensor because of the presence of the space rotation A_{ik} in the formula. Nevertheless its generalization gives the chr.inv.-tensor

$$C_{lkij} = \frac{1}{4}\left(H_{lkij} - H_{jkil} + H_{klji} - H_{iljk}\right),$$

which possesses all the algebraic properties of the Riemann-Christoffel tensor in this three-dimensional space and, at the same time, the property of chronometric invariance. Therefore Zelmanov called C_{iklj} the *chr.inv.-curvature tensor* the tensor of the observable curvature of the observer's spatial section. Its successive contraction

$$C_{kj} = C_{kij\cdot}^{\cdots i} = h^{im} C_{kimj}\,, \qquad C = C_j^j = h^{lj} C_{lj}$$

gives the chr.inv.-scalar C, which is the *observable three-dimensional curvature* of this space.

Chr.inv.-projections of the Riemann-Christoffel tensor

$$X^{ik} = -c^2\frac{R_{0\cdot 0\cdot}^{\cdot i\cdot k}}{g_{00}}\,, \quad Y^{ijk} = -c\,\frac{R_{0\cdots}^{\cdot ijk}}{\sqrt{g_{00}}}\,, \quad Z^{ijkl} = c^2 R^{ijkl},$$

after substituting the necessary components of the Riemann-Christoffel tensor and lowering indices, are

$$X_{ij} = \frac{^*\partial D_{ij}}{\partial t} - \left(D_i^l + A_{i\cdot}^{\cdot l}\right)\left(D_{jl} + A_{jl}\right) + \frac{1}{2}\left(^*\nabla_i F_j + {}^*\nabla_j F_i\right) - \frac{1}{c^2}\,F_i F_j\,,$$
$$Y_{ijk} = {}^*\nabla_i\left(D_{jk} + A_{jk}\right) - {}^*\nabla_j\left(D_{ik} + A_{ik}\right) + \frac{2}{c^2}\,A_{ij} F_k\,,$$
$$Z_{iklj} = D_{ik} D_{lj} - D_{il} D_{kj} + A_{ik} A_{lj} - A_{il} A_{kj} + 2A_{ij} A_{kl} - c^2 C_{iklj}\,,$$

where we have $Y_{(ijk)} = Y_{ijk} + Y_{jki} + Y_{kij} = 0$, just like the Riemann-Christoffel tensor. Successive contraction of the spatial observable projection Z_{iklj} gives

$$Z_{il} = D_{ik} D_l^k - D_{il} D + A_{ik} A_{l\cdot}^{\cdot k} + 2A_{ik} A_{\cdot l}^{k\cdot} - c^2 C_{il}\,,$$
$$Z = h^{il} Z_{il} = D_{ik} D^{ik} - D^2 - A_{ik} A^{ik} - c^2 C\,.$$

Accordingly, Einstein's equations in the case where matter is arbitrarily distributed throughout the space have the chr.inv.-projections (the chr.inv.-Einstein equations)

$$\frac{^*\partial D}{\partial t} + D_{jl} D^{jl} + A_{jl} A^{lj} + \left(^*\nabla_j - \frac{1}{c^2}\,F_j\right) F^j = -\frac{\kappa}{2}\left(\rho c^2 + U\right) + \lambda c^2,$$

$$^*\nabla_j\left(h^{ij} D - D^{ij} - A^{ij}\right) + \frac{2}{c^2}\,F_j\,A^{ij} = \kappa J^i,$$

$$\frac{^*\partial D_{ik}}{\partial t} - \left(D_{ij} + A_{ij}\right)\left(D_k^j + A_{k\cdot}^{\cdot j}\right) + D D_{ik} + 3A_{ij} A_{k\cdot}^{\cdot j} - \frac{1}{c^2}\,F_i F_k + {}$$
$$+ \frac{1}{2}\left(^*\nabla_i F_k + {}^*\nabla_k F_i\right) - c^2 C_{ik} = \frac{\kappa}{2}\left(\rho c^2 h_{ik} + 2U_{ik} - U h_{ik}\right) + \lambda c^2 h_{ik}\,.$$

where $^*\nabla_j$ denotes the chr.inv.-derivative, for instance

$$^*\nabla_i\, q_k = \frac{^*\partial q_k}{dx^i} - \Delta_{ik}^l q_l\,, \quad {}^*\nabla_i\, q^k = \frac{^*\partial q^k}{dx^i} + \Delta_{il}^k q^l,$$
$$^*\nabla_i\, q_{jk} = \frac{^*\partial q_{jk}}{dx^i} - \Delta_{ij}^l q_{lk} - \Delta_{ik}^l q_{jl}\,,$$
$$^*\nabla_i\, q_j^k = \frac{^*\partial q_j^k}{dx^i} - \Delta_{ij}^l q_l^k + \Delta_{il}^k q_j^l\,,$$
$$^*\nabla_i\, q^{jk} = \frac{^*\partial q^{jk}}{dx^i} + \Delta_{il}^j q^{lk} + \Delta_{il}^k q^{jl},$$
$$^*\nabla_i\, q^i = \frac{^*\partial q^i}{\partial x^i} + \Delta_{ji}^j q^i = \frac{^*\partial q^i}{\partial x^i} + \frac{^*\partial \ln\sqrt{h}}{\partial x^i}\, q^i,$$
$$^*\nabla_i\, q^{ji} = \frac{^*\partial q^{ji}}{\partial x^i} + \Delta_{il}^j q^{il} + \frac{^*\partial \ln\sqrt{h}}{\partial x^i}\, q^{ji},$$

while the quantities

$$\rho = \frac{T_{00}}{g_{00}}\,, \qquad J^i = \frac{c\,T_0^i}{\sqrt{g_{00}}}\,, \qquad U^{ik} = c^2 T^{ik}$$

(from which we have $U = h^{ik} U_{ik}$) are the chr.inv.-components of the energy-momentum tensor $T_{\alpha\beta}$ of distributed matter: the physical observable density of the field energy ρ, the physical observable density of the field momentum vector J^i, and the physical observable stress-tensor U^{ik}. For instance, the energy-momentum tensor of the electromagnetic field has the form [20]

$$T_{\alpha\beta} = \frac{1}{4\pi}\left(-F_{\alpha\sigma} F_{\beta\cdot}^{\cdot\sigma} + \frac{1}{4}\,F_{\mu\nu} F^{\mu\nu} g_{\alpha\beta}\right),$$

where $F_{\alpha\beta}$ is the electromagnetic field tensor (so-called Maxwell's tensor). (It follows that the field density ρ is connected to the quantity $U = h^{ik} U_{ik}$ by $\rho c^2 = U$.)

In this way, for any quantity or equation obtained using general covariant methods, we can calculate their physically observable projections on the time line and the spatial section of any particular reference body and formulate the projections in terms of their real physically observable properties, from which we obtain equations containing only quantities measurable in practice.